Advances in Terahertz Spectroscopy Nano-scanner and Sub-surface 3D Imaging for Biomaterial

Anis Rahman and Aunik K Rahman

Applied Research & Photonics

http://arphotonics.net

Presented at the

6th International Conference and Exhibition on Biosensors & Bioelectronics

September 22-23, 2016 Phoenix, USA

Plan

- Intro to terahertz
- Integrated terahertz nano-scanning spectrometer
- Examples of spectral analysis
- Principle of non-destructive imaging
- Examples: sub-surface imaging @ 1 nm resolution
- 3D imaging of Cr^3 nano-particles, semiconductor, quantum dots, etc.
- Layer by layer inspection
- Conclusions

Introduction

- **Terahertz is able to penetrate most non-metalic objects → sub-surface scanning**
- **It is non-ionizing → allows, non-destructive probing**
- **Penetrates → Sub-surface, interior of multi-layered composite**
- **Nano-scale diagnosis of semiconductor wafer, paint, coatings, soft tissue, etc.**

Motivation

- Deploying Terahertz to inspect under the surface
- To achieve 1 nm resolution
- Non-destructive, non-contact
- layer by layer imaging and spectral analysis
- Characterize 2D and 3D nanomaterials

Terahertz

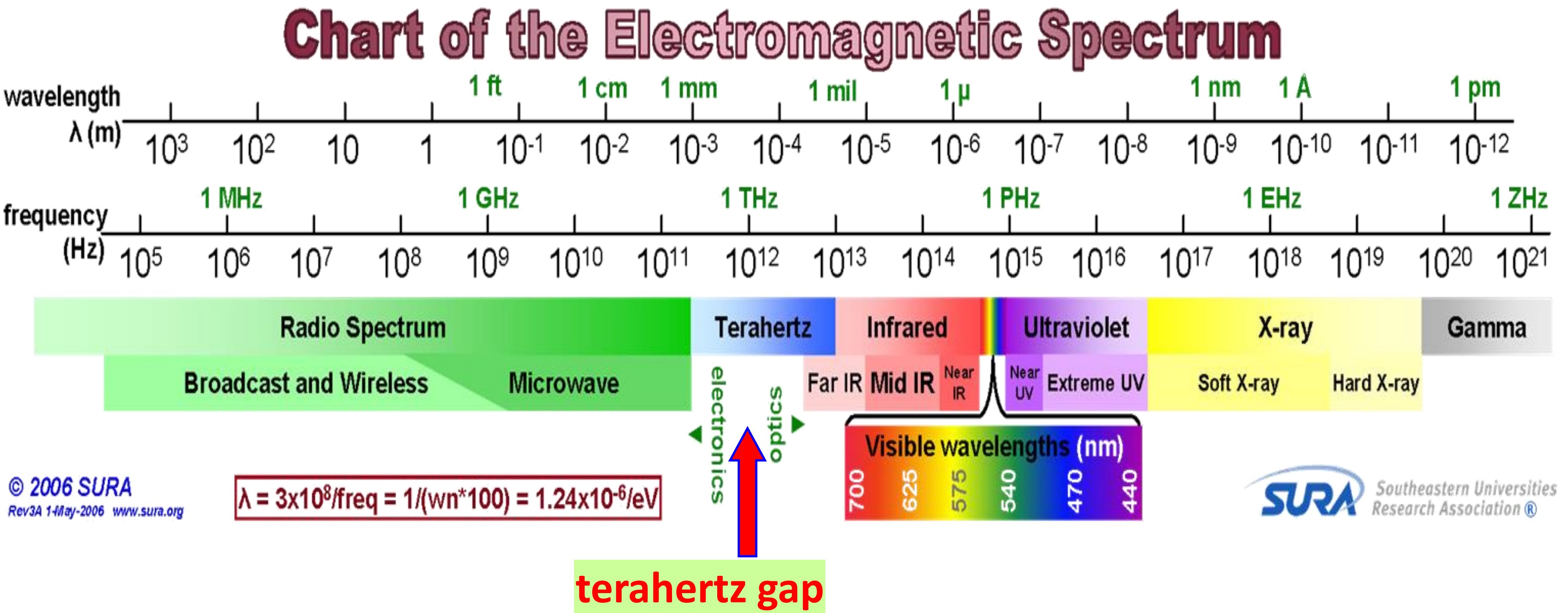

Raman/IR covers ~250 to 4000 cm^{-1} → Bond, torsion

THz covers 0.1 THz to ~35 THz (from ~3 to 1200 cm^{-1})
→ All kinds of resonances, Molecular backbone, intermolecular interaction

Terahertz generation

Technology	Advantages	Challenges
Electro-optic rectification (EOR)	• Easy alignment • Broadband spectrum	• Needs femto-s pulsed laser • Limited output power • Higher cost, Low efficiency
Difference Frequency Gen. (DFG)	• Tunable, Pulsed or CW • Higher power (~mW) • Broadband or narrow	• Two lasers needed • Difficult alignment • Needs high $\chi^{(2)}$ material
Dendrimer dipole excitation (DDE) → ARP	• No pulsed laser, no high voltage • Tunable output power & range	• New technology • Dendrimer doping and poling
Photo-conductor	• Legacy technology	• Low output power, ~μW • High voltage & pulsed laser • Limited THz range
Reactor Synchrotron	• Higher output power	• Huge in size and cost • Limited THz range • Needs dedicated facility
QCL	• No pump laser	• Unstable, fixed bandwidth, low power, not tunable, fab

Difference Frequency Generation

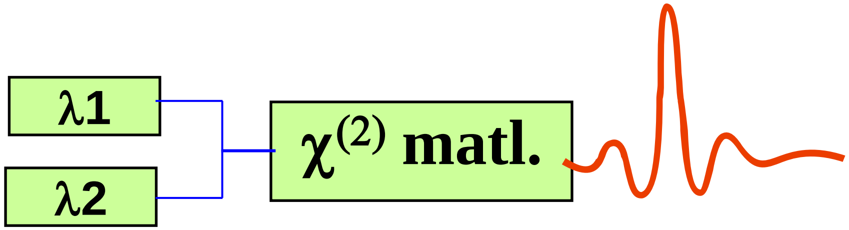

$$f_{THz} \propto \nu_2 - \nu_1$$

THz power ↑ as $\chi^{(2)}$ ↑

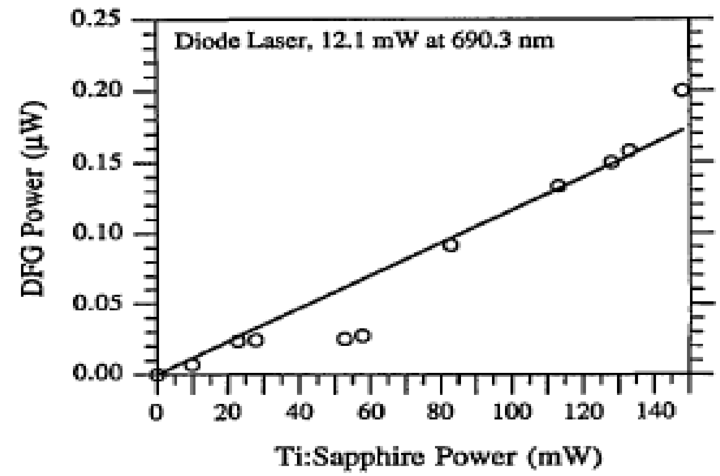

Setup of Simon et al., 1993

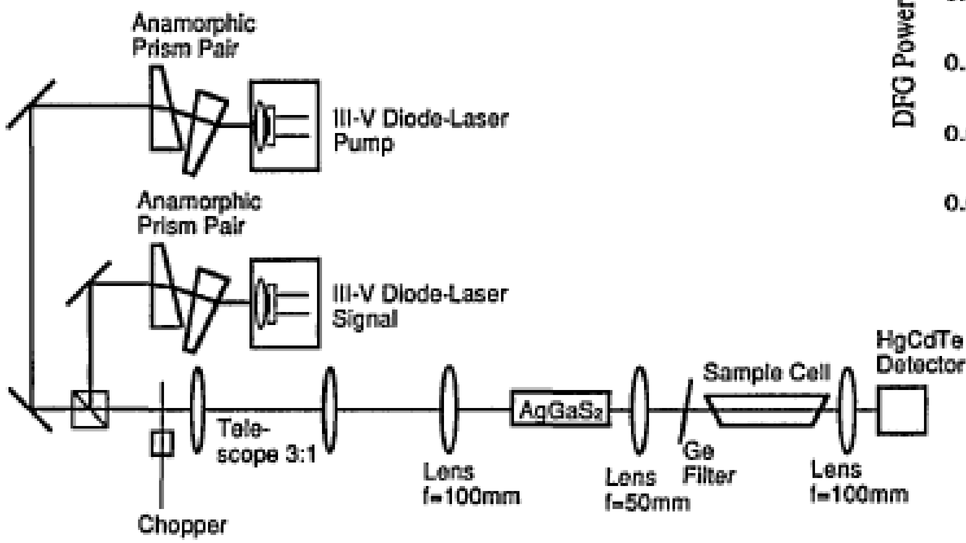

Difference Frequency

Ref: U. Simon, C. E. Miller, C. C. Bradley, R. G. Hulet, **R. F. Curl,** and F. K. Tittel, “Difference-frequency generation in $AgGaS_2$ by use of single-mode diode-laser pump sources,” OPTICS LETTERS Vol. 18, No. 13 / July 1, 1993, p 1062–1064.

Electro-optic Dendrimer

- The terminal groups each have two sites available for dopant
- A distribution of dipoles expected via chromophore doping.

$$\mu = ql$$

$$\boxed{\Rightarrow\ \mu(x) = ql(x)}$$

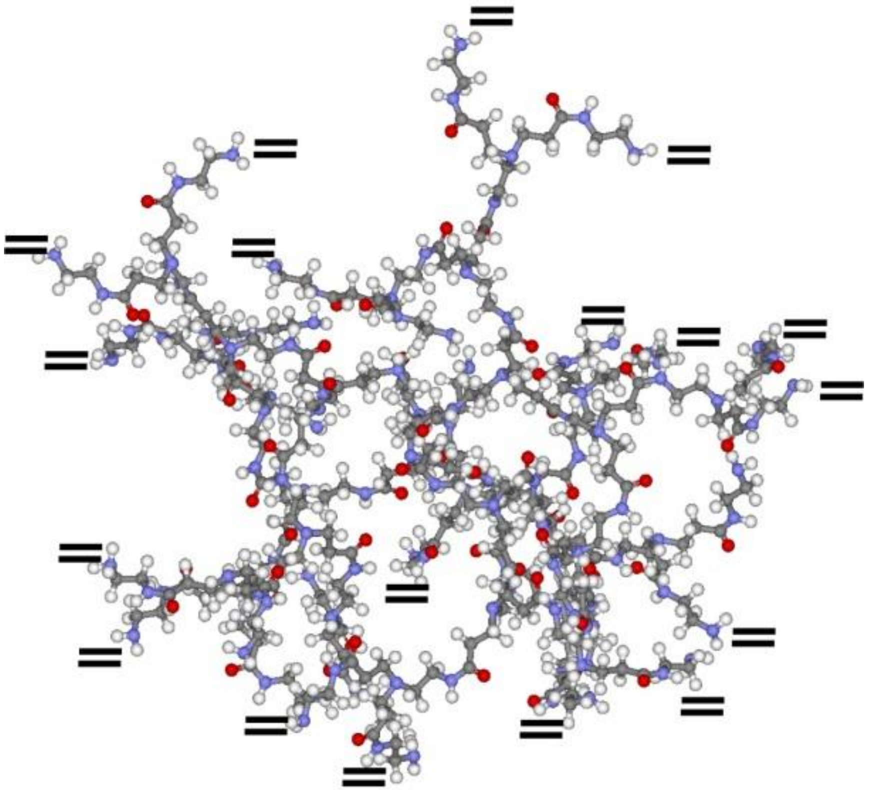

Molecular structure of a dendrimer (generation 3)

Electro-optic Dendrimer

- $w_{THz} \propto \chi^{(2)} w_{pump}^2$
- **THz power ↑ as $\chi^{(2)}$ ↑**
- $\chi^{(2)} = nf\beta\langle\cos^3\theta\rangle$

n dipole density

f local field factor

β average hyperbolarizability

θ dipole alignment angle

- **There are many chromophores to choose from**

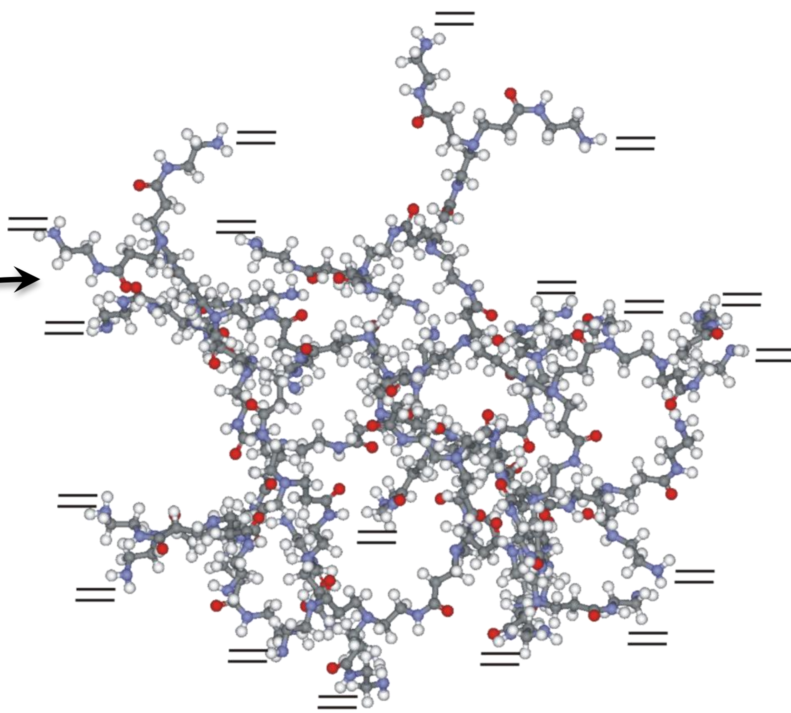

Dendrimer Dipole Excitation (DDE)

- Energy level diagram of dendrimer resulting from chromophore doping and poling
- A distribution of dipole moments creates CW broadband emission via DDE.
- No separate dispersion element needed
- Multispectral imaging

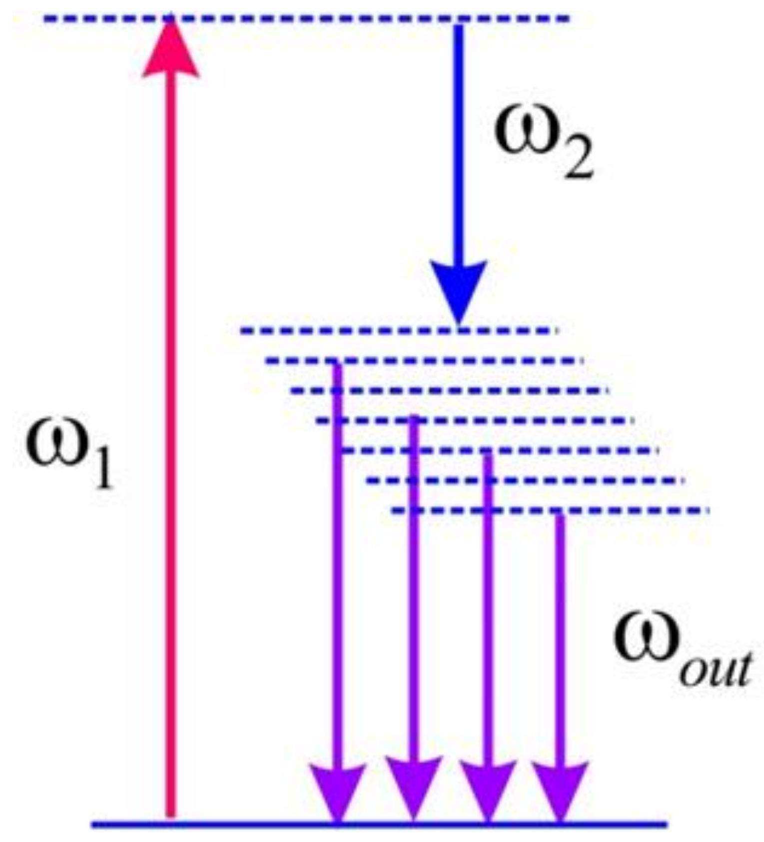

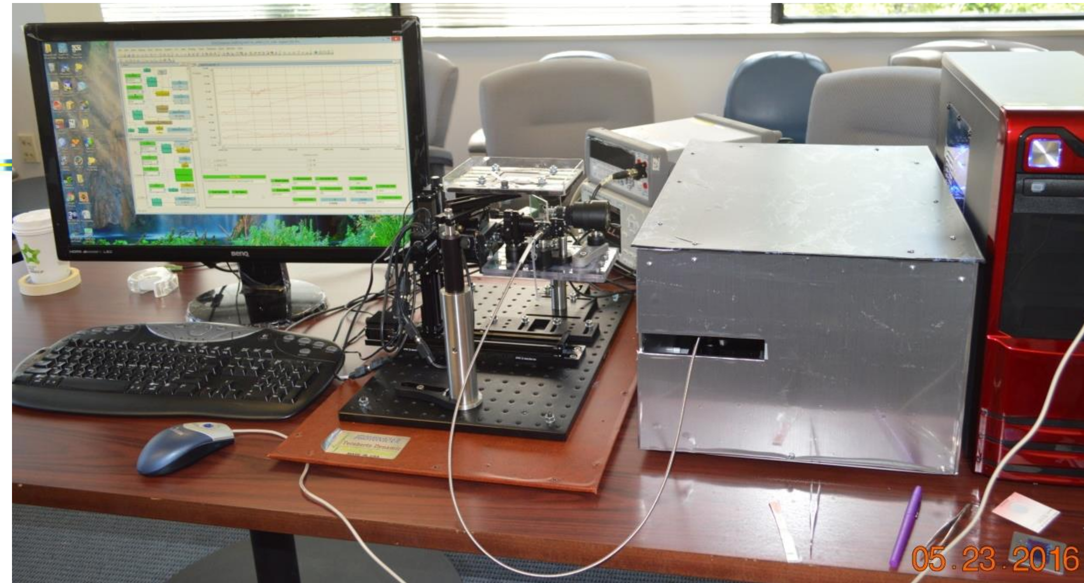

Live demo in booth #734

Principle of THz Spectroscopy

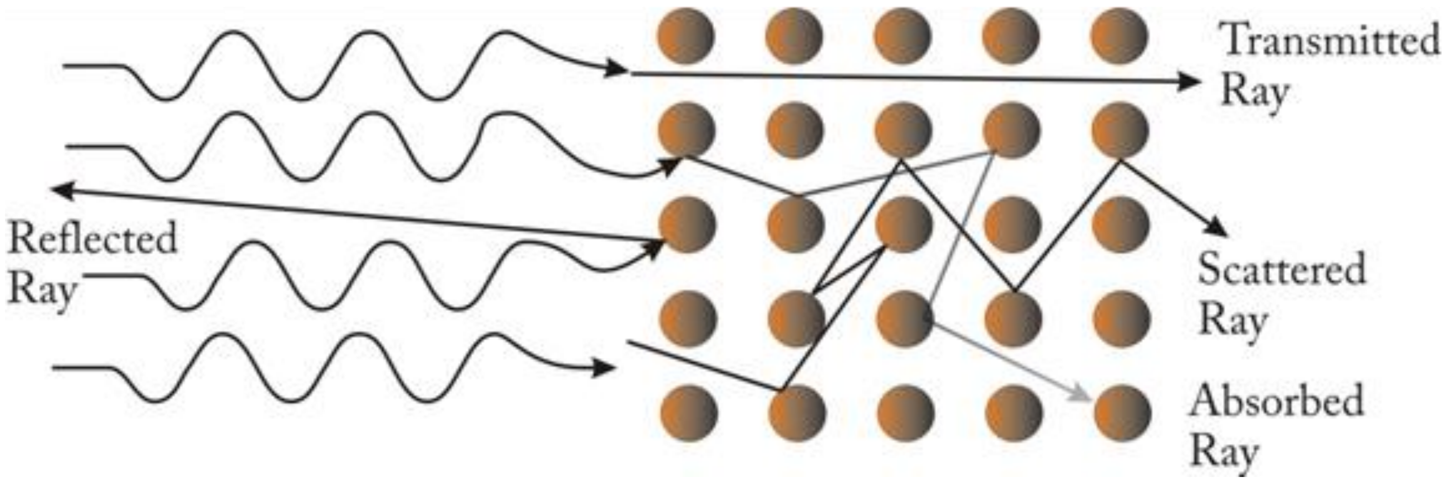

- THz radiation may stimulate many resonances such as molecular vibrations (in general molecular "events"), resulting in the THz photons being affected by characteristic amounts determined by a specific interaction or event.
- The change in energy yields information about the molecular nature of the interaction.
- Infrared and Raman spectroscopy yields similar information but not capable of detecting many resonant states as can be detected with THz.
- Spontaneous Raman scattering is typically very weak, as a result the main difficulty of Raman spectroscopy is in resolving the weak inelastically scattered light from the intense Rayleigh scattered laser light.

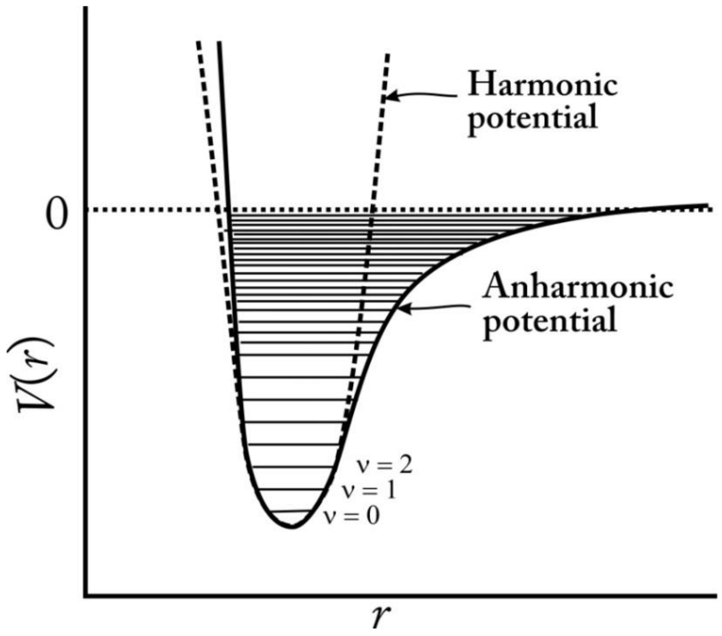

Potential energy of a diatomic molecule as a function of displacement during a vibration

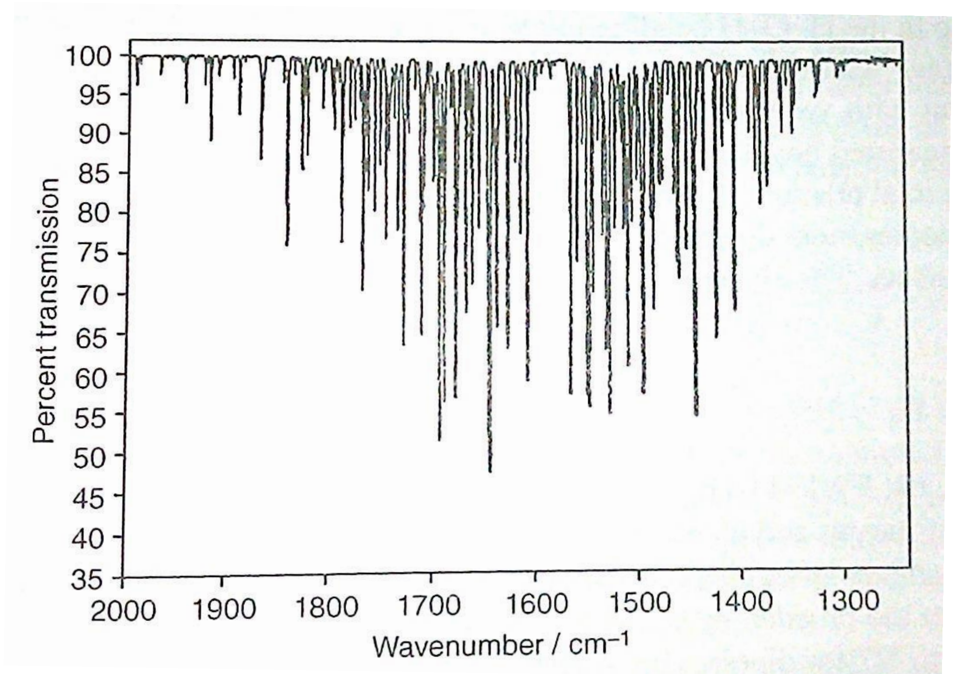

Vibration-rotation spectrum of H-O-H bending mode of water vapor

Higher sensitivity is required to sense more "states"

Ref: Griffiths & de Haseth, Fourier Transform Infrared Spectroscopy, Wiley 2007

Terahertz penetrates

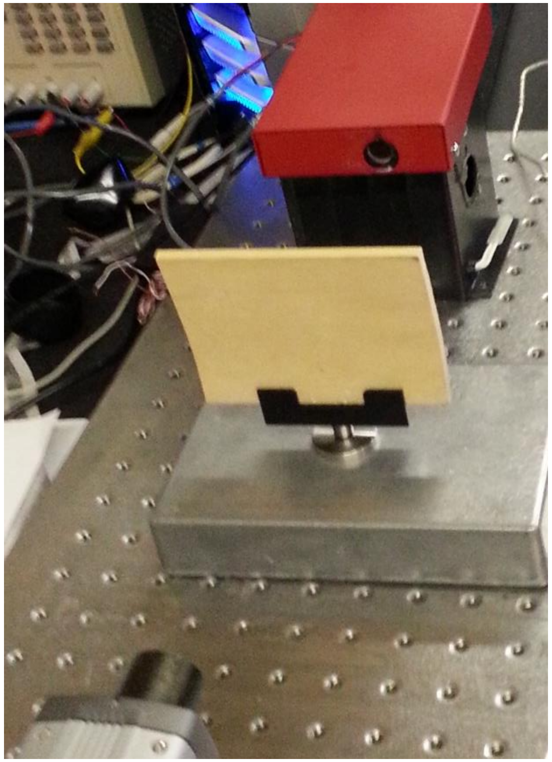

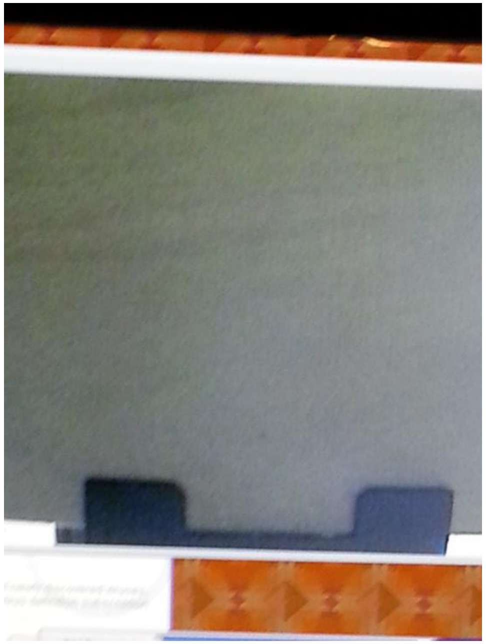

Terahertz penetrates through wood plank and other non-metallic objects
→ Applications in security and screening

Spectrometer Validation

Water vapor absorption spectrum obtained using the THz spectrometer compared to that calculated using the HITRAN database by the NIST. An expanded portion in the panel (b) containing pressure broadened water lines from NIST (c): Expanded view of vapor absorption lines obtained from ARP's TeraSpectra (see Fig. 5). Low frequency peaks match well with those reported by the NIST [1].

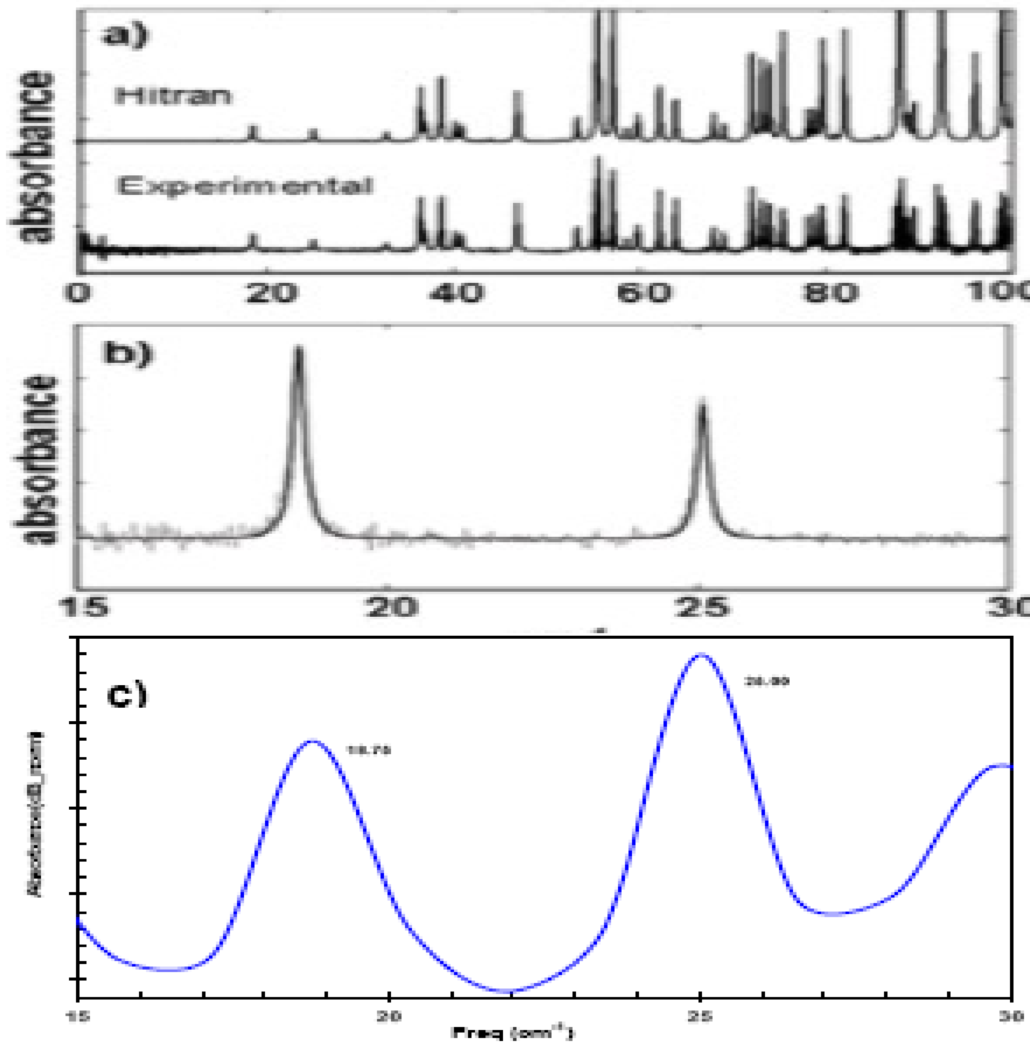

1. http://arphotonics.net/WaterVaporComparison1.pdf

water spectrum

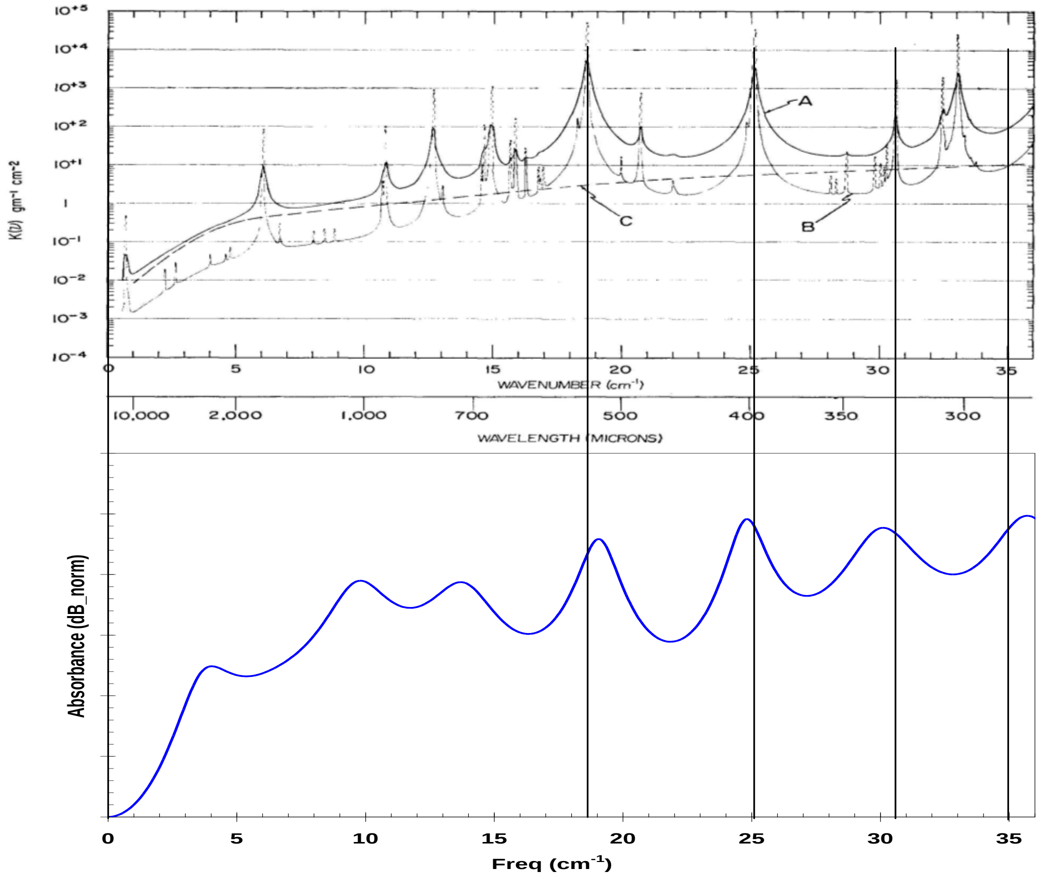

Ref. Darrell Burch, "Absorption of Infrared Radiant Energy by CO2 and H2O. III. Absorption by H_2O between 0.5 and 36 cm^{-1} (278 u-2 cm)," Journal of the Optical Society of America, 58 (#10), 1383, 1968.

Water spectrum up to 40 THz

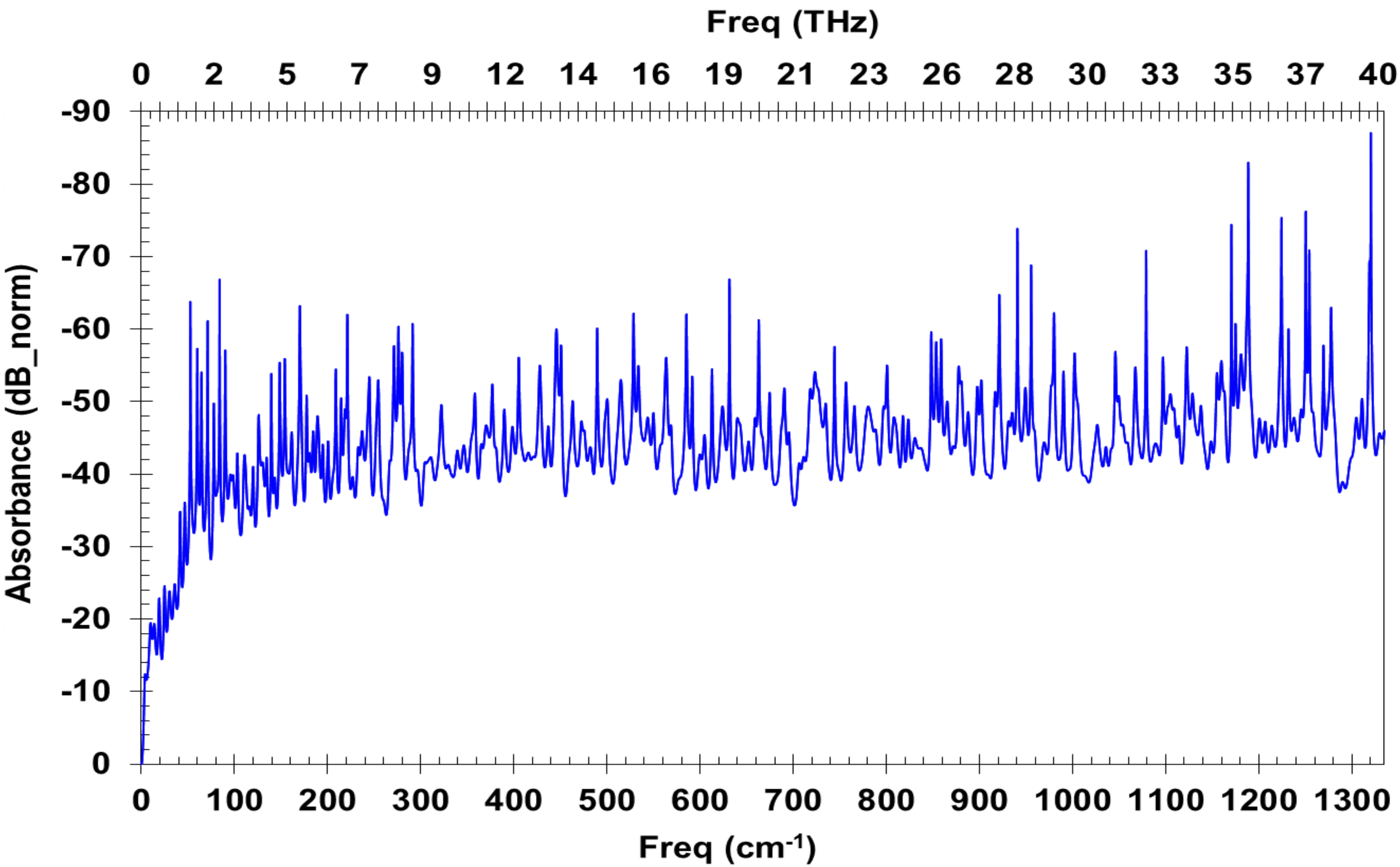

Validation from JLC group

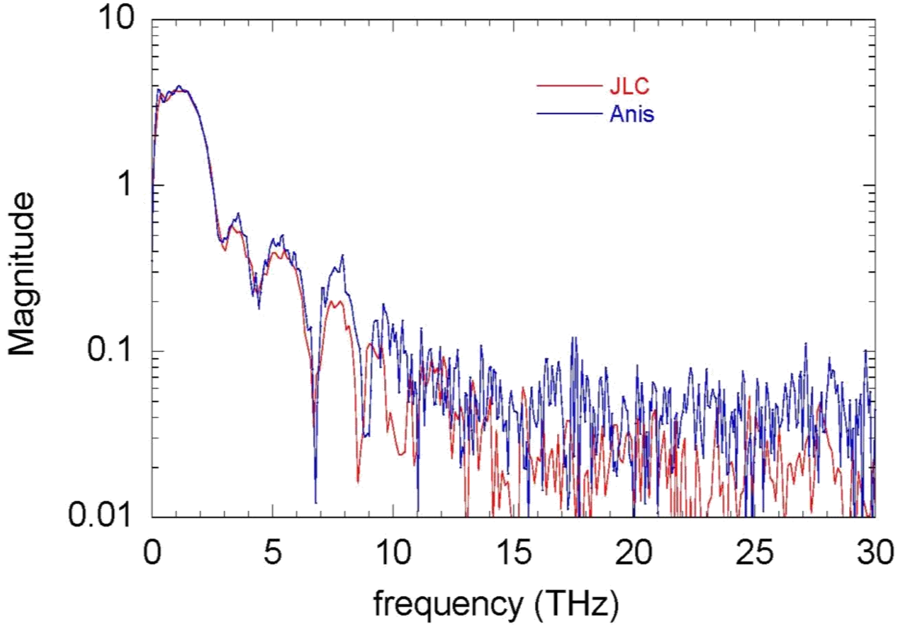

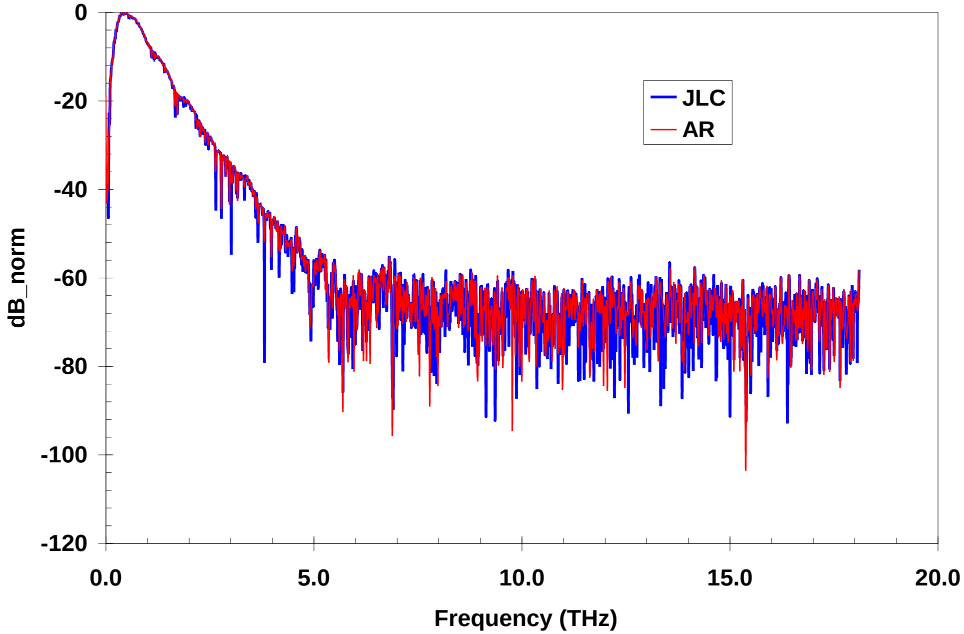

ARP data validated by Prof. Coutaz

JLC data overlaps with ARP data

PE time-domain spectrum

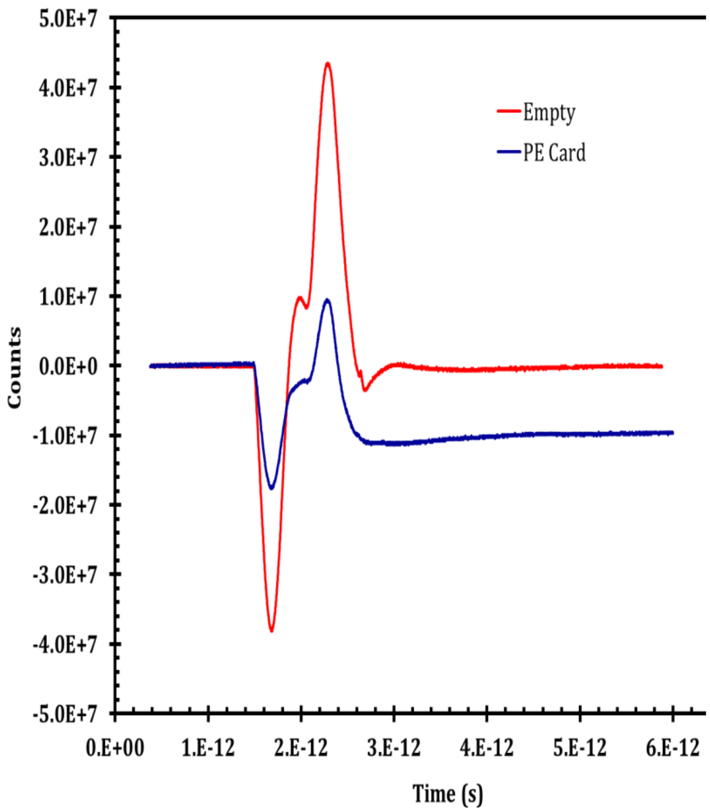

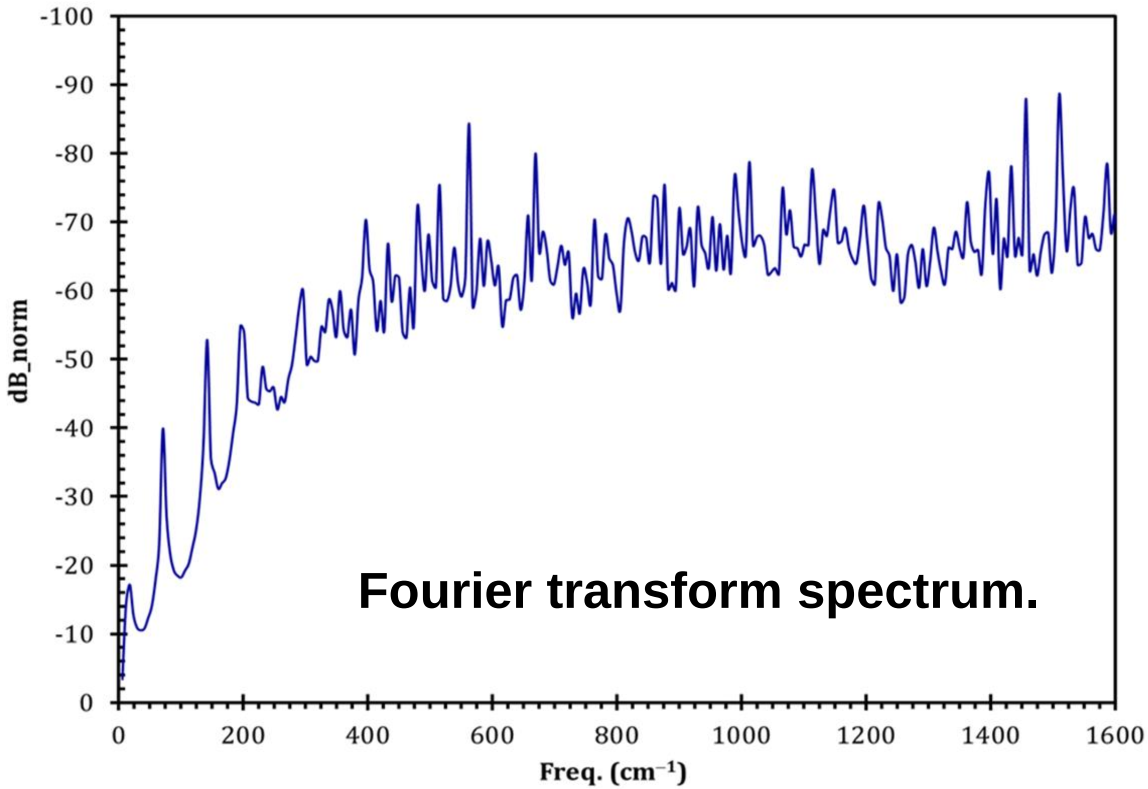

- **TeraSpectra reproduced absorbance peaks known from other methods**
- **Many peaks not visible previously were discovered.**

Polyethylene comparison

Source	Reported (1/cm)	TeraSpectra (1/cm)
Sigma-Aldrich [7]	70.8	71
FreeSnell [6]	723.3	722.5
	749.5	746.2
	1466.02	1457, 1469
	1492.23	1486.4 1510.0

[7] Polyethylene spectrophotometric grade,SIGMA-ALDRICH. http://thzdb.org/image.php?image=000000773

[6] FreeSnell: Polyethylene http://people.csail.mit.edu/jaffer/FreeSnell/polyethylene.html

DHS Test Sample

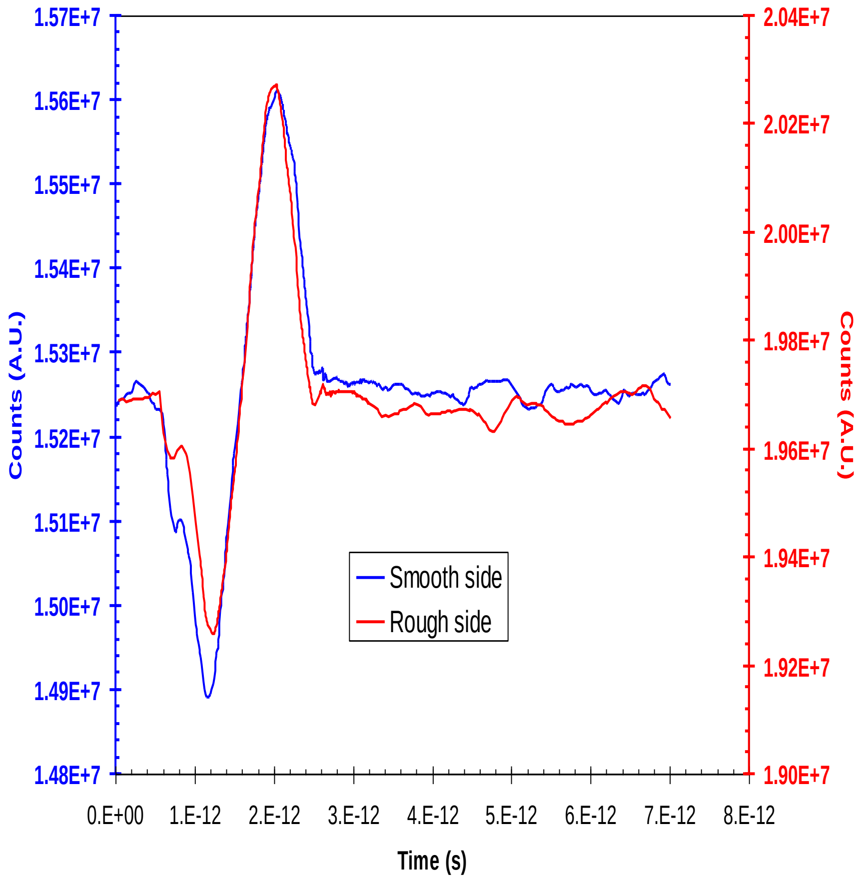

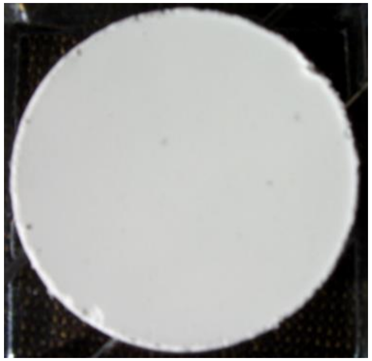

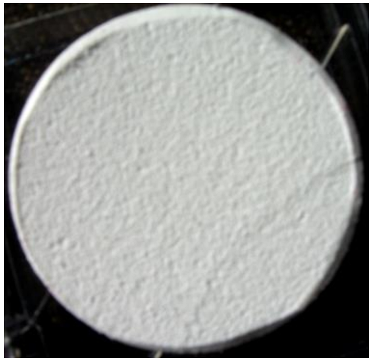

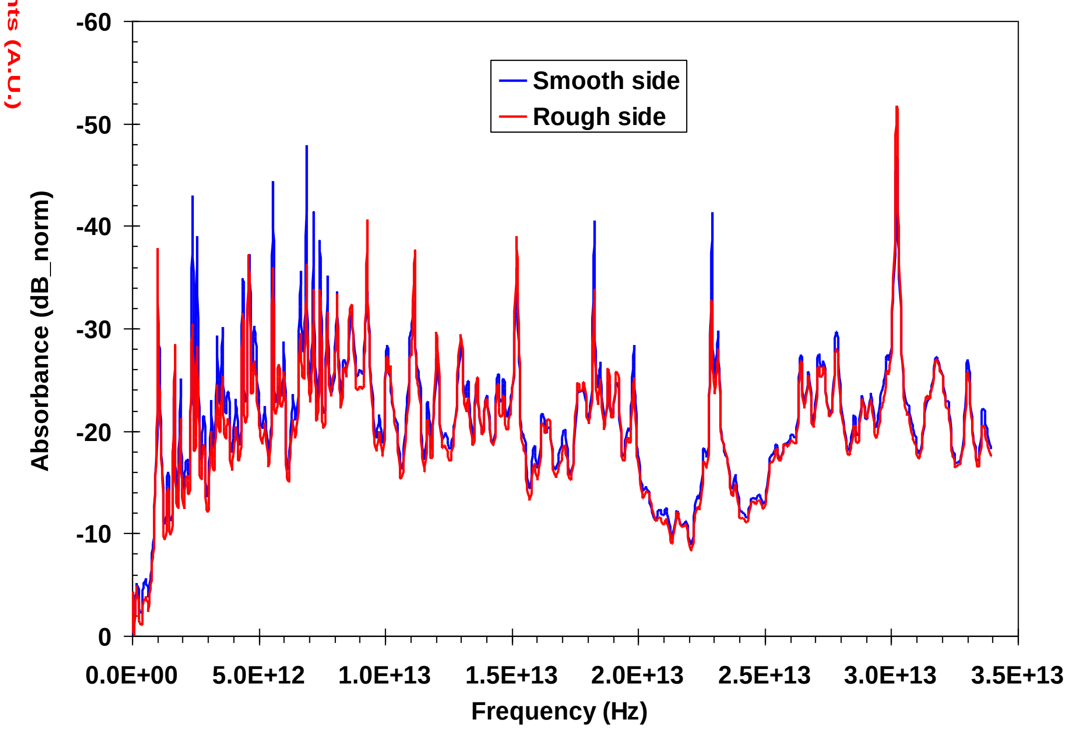

Spectra of skin samples

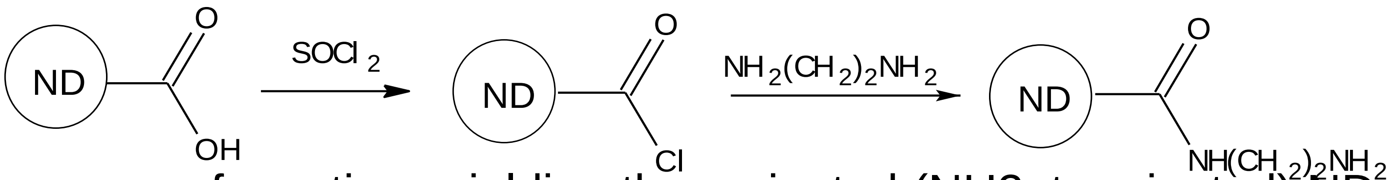

The sequence of reactions yielding the aminated (NH2–terminated) ND: ND-EDA (Ethylenediamine).

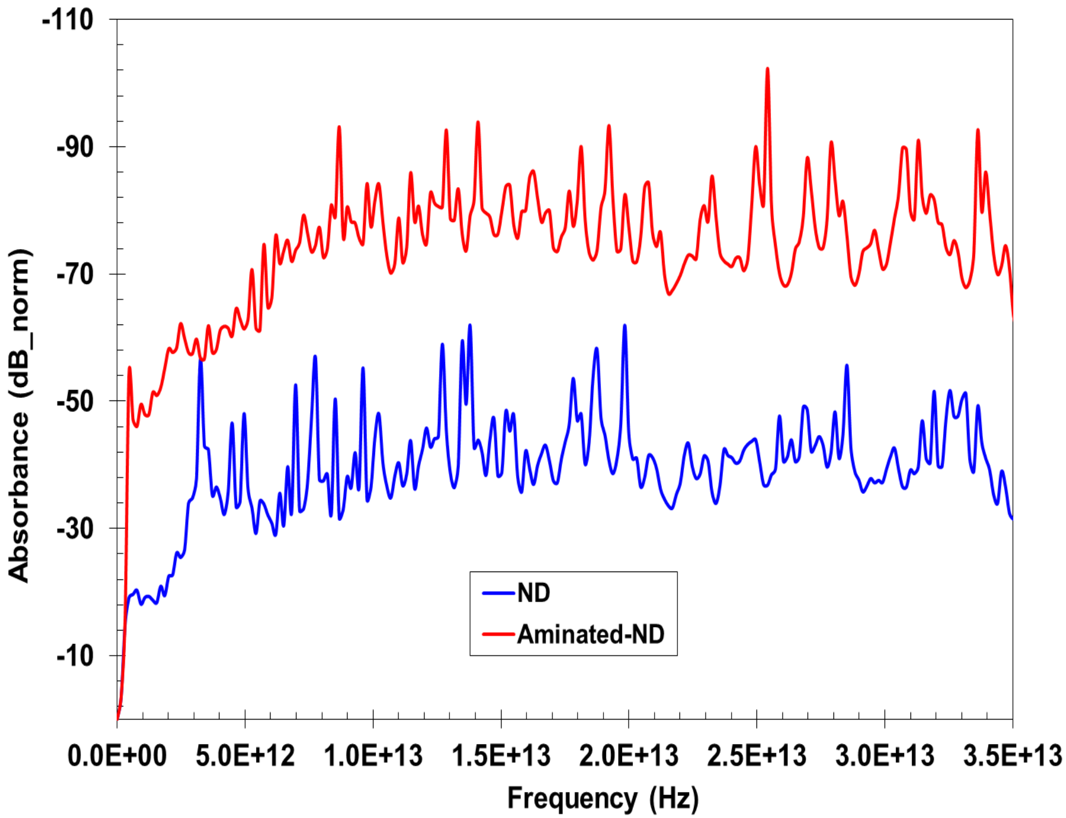

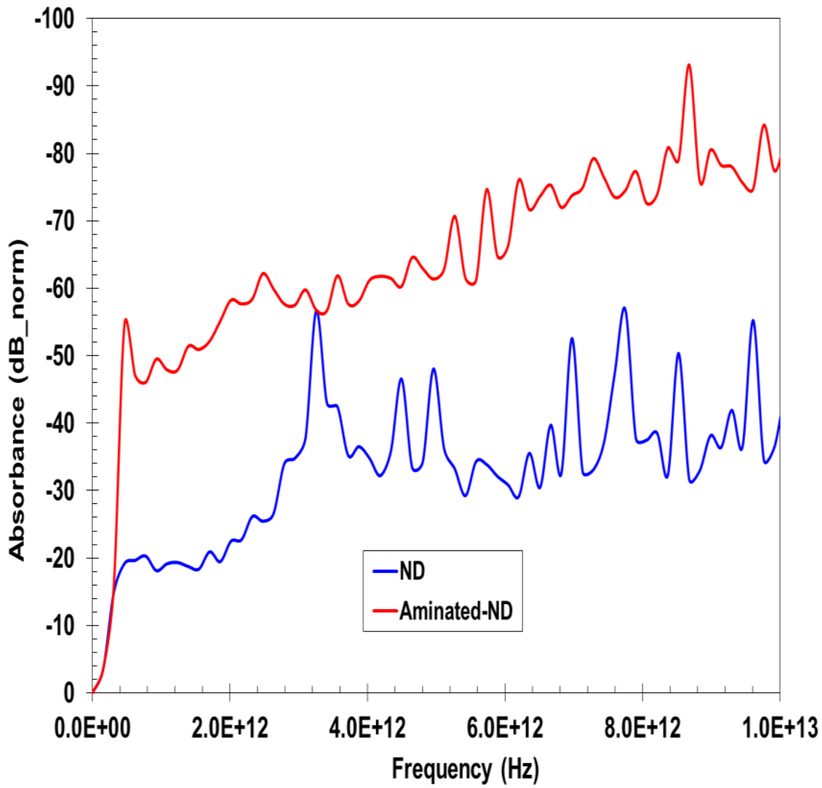

Wafer spectra

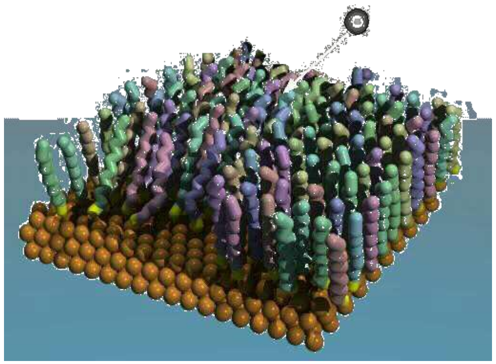

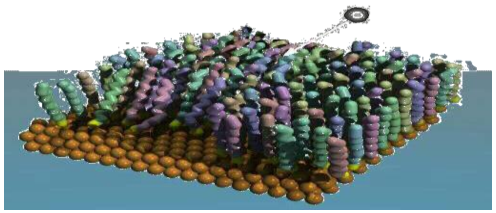

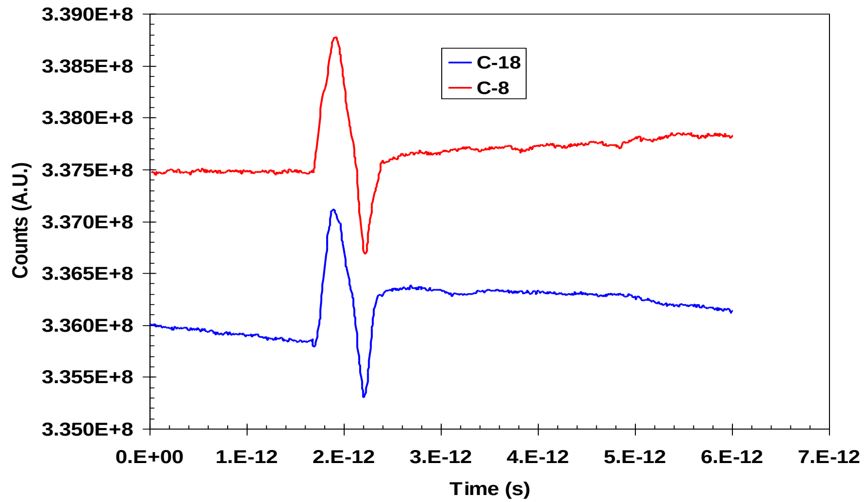

To determine differences between two SAMs on silicon wafer surface:

(1) n-Octadecyltrichlorosilane: (C18), Mw = 387.93 g/mol
Formula: CH3(CH2)17SiCl3

(2) 7-OCT-1-Enyltrichlorosilane: (C8)
Mw = 245.65 g/mol
Formula:H2C=CH(CH2)6SiCl3
Samples courtesy of UC Irvine

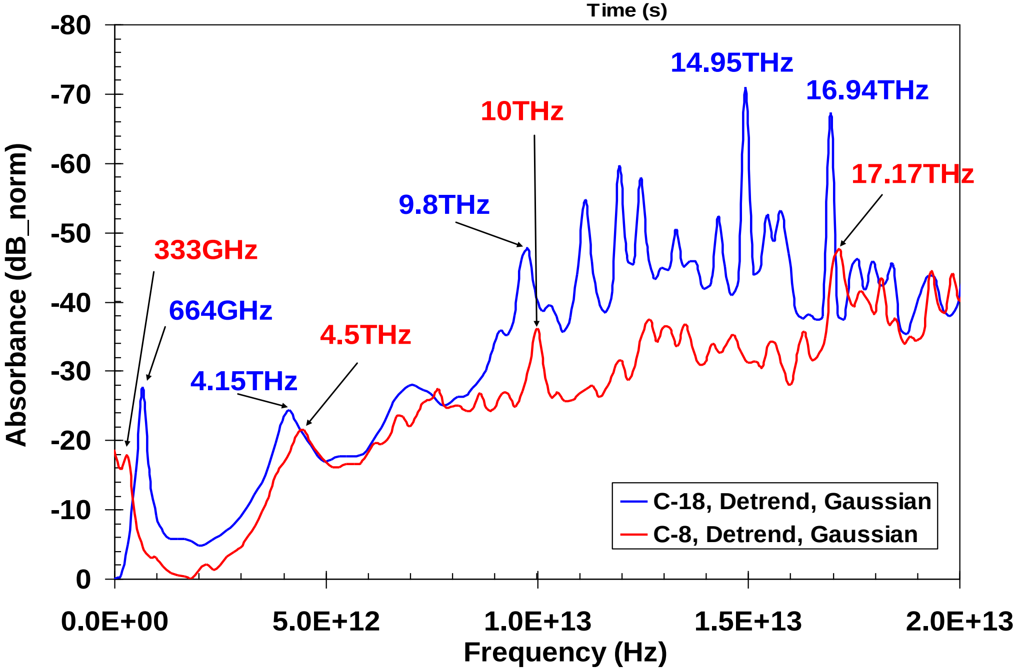

Skin spectra

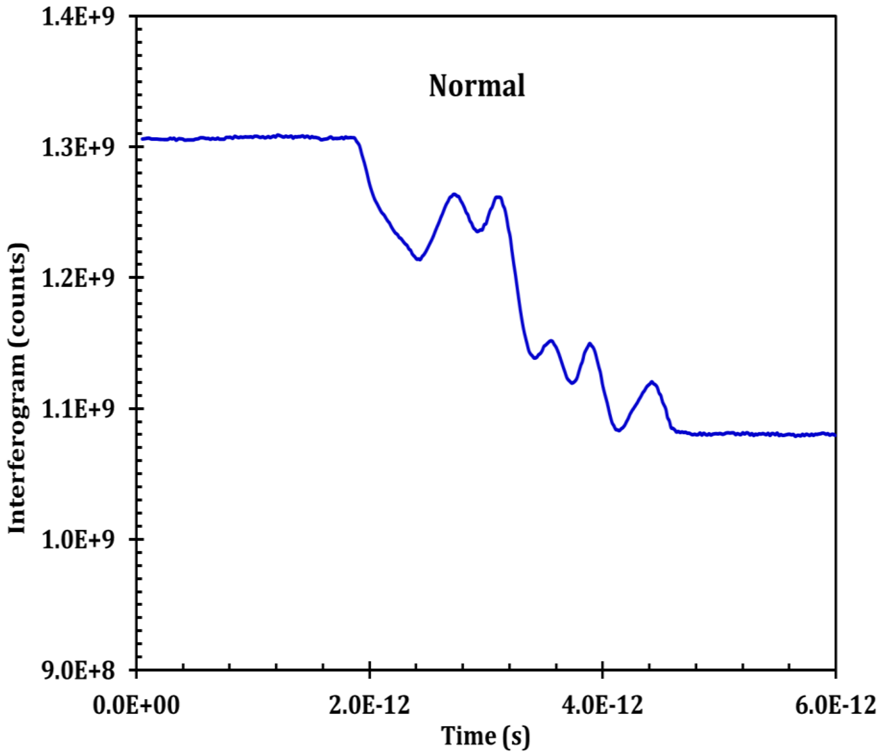

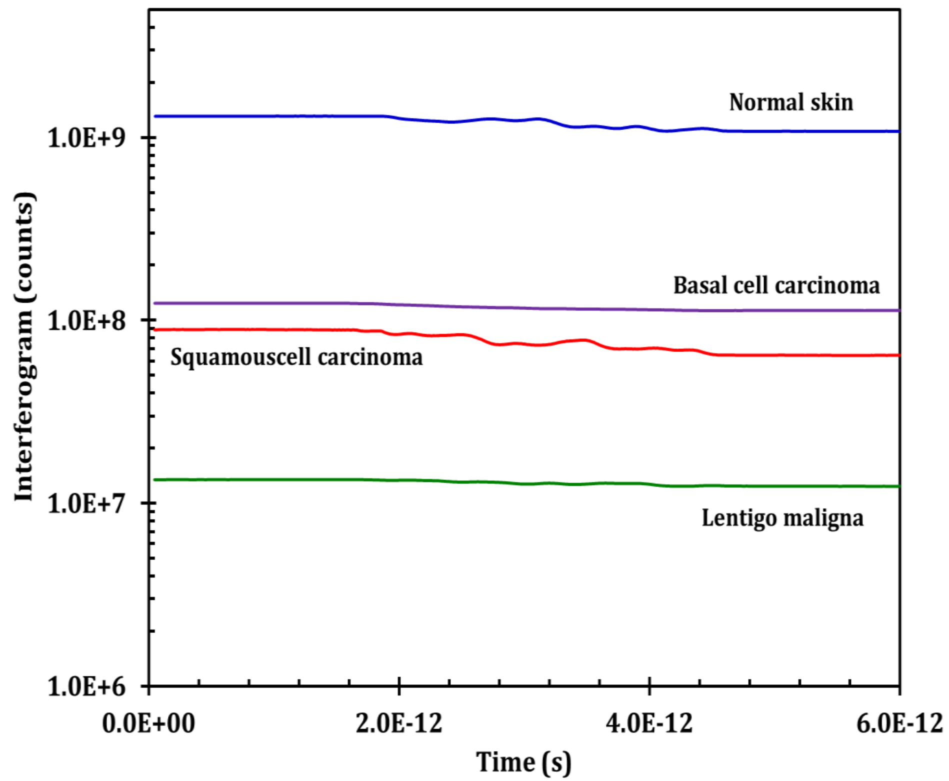

Measured time-domain signal (interferogram) of skin samples with conditions. Left: healthy skin. Right: healthy, BCC, SCC, Lentigo

Absorbance spectra of 4 skins

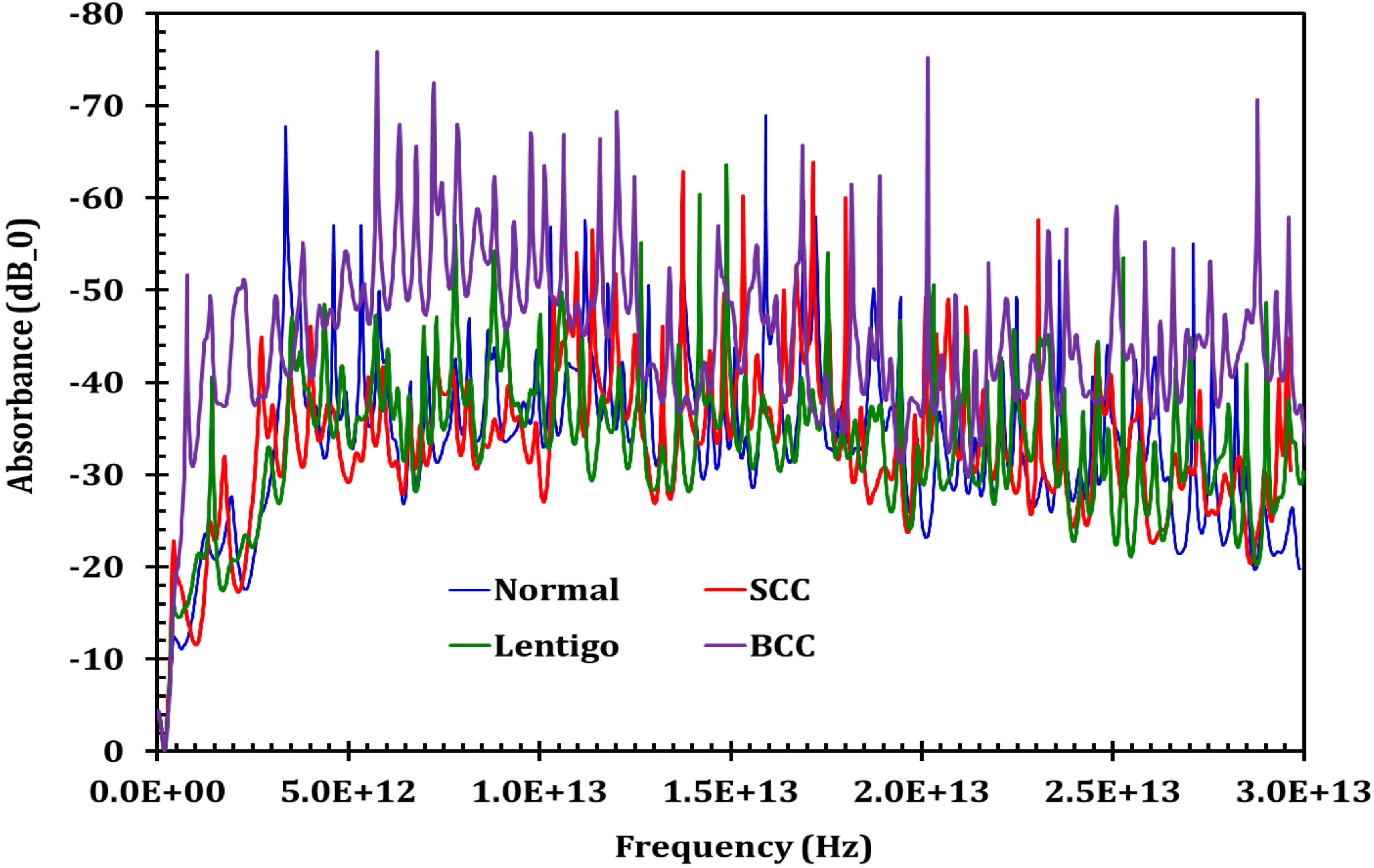

Absorbance spectra close-up

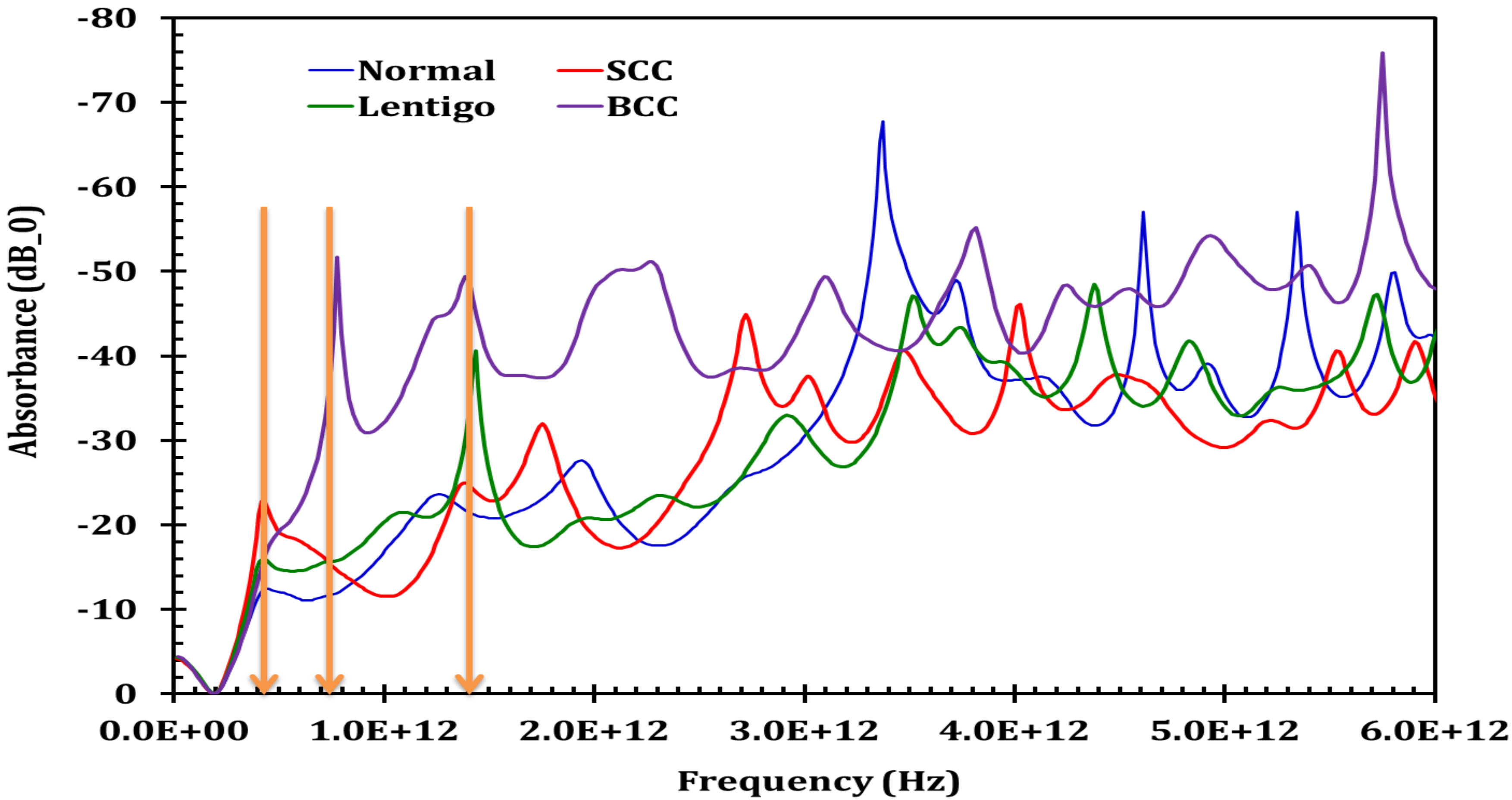

Known water peaks are present. Others peaks may be assigned to the skin condition.

Layer by layer spectra

Sample: Ge over Silicon

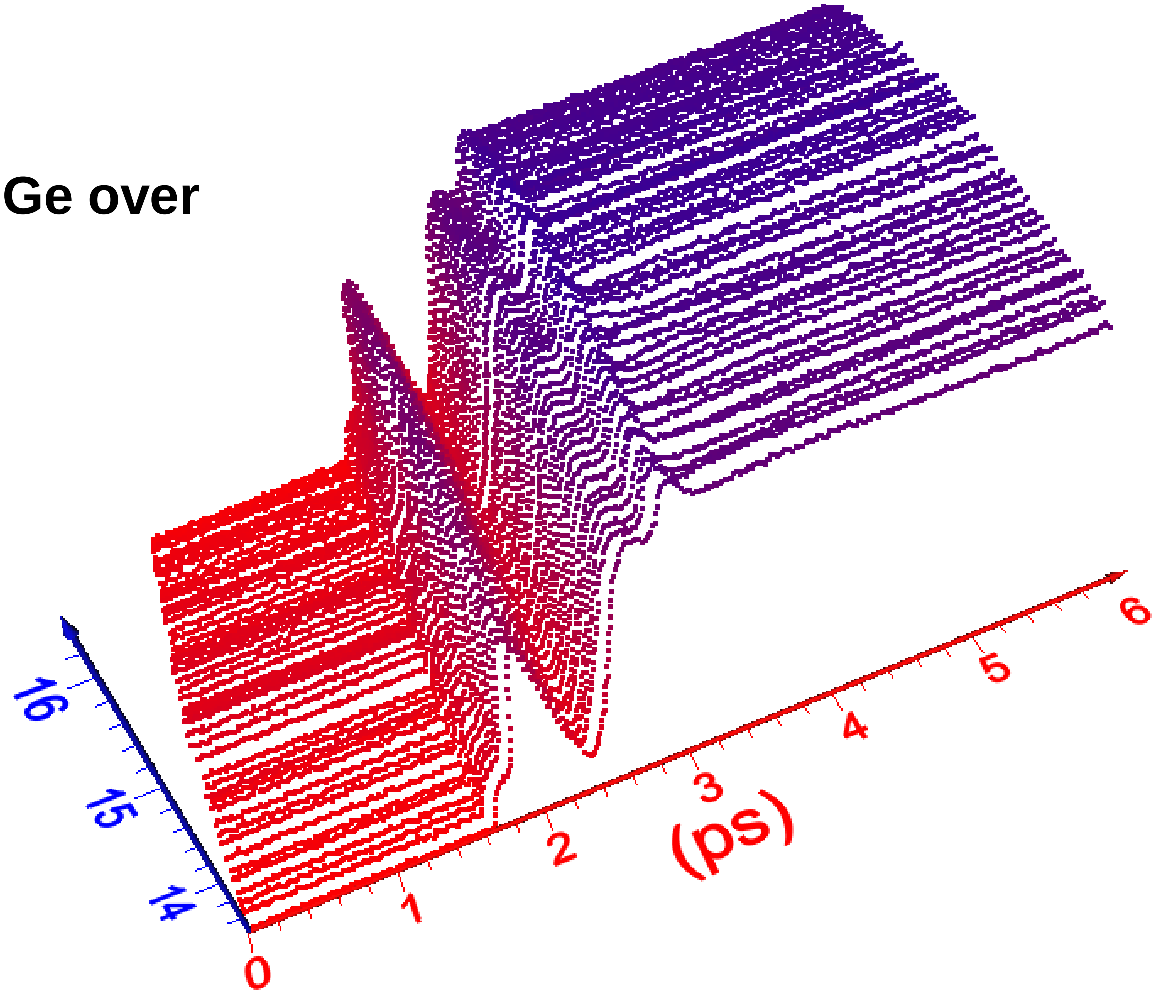

Reconstructive Imaging

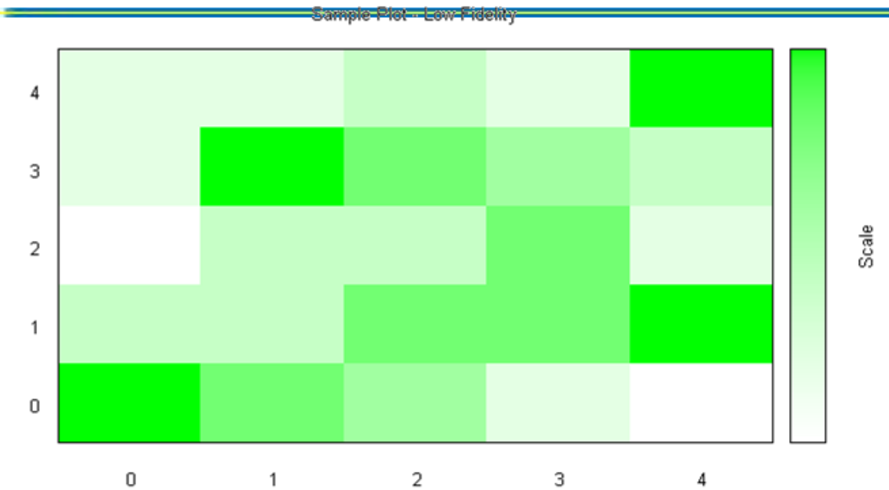

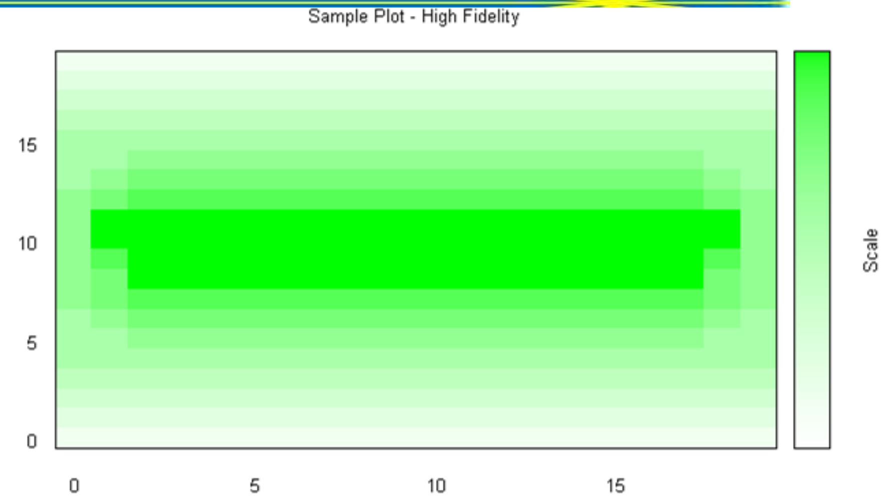

Potential products

- **THz Coherent Tomography**
- **Skin/tissue imaging**
- **Early stage cancer detection**

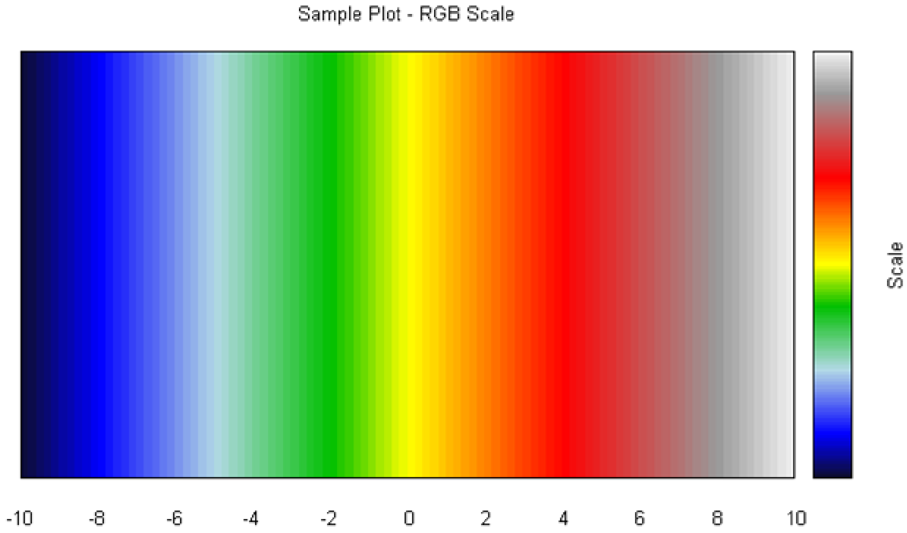

Gridding with Inverse Distance to Power Equations

$$\widehat{\boldsymbol{C}}_{\boldsymbol{j}} = \frac{\sum_{i=1}^{n} \frac{C_i}{h_{ij}^{\beta}}}{\sum_{i=1}^{n} \frac{1}{h_{ij}^{\beta}}} \qquad (1)$$

where, $h_{ij} = \sqrt{d_{ij}^2 + \delta^2}$,

h_{ij} is the effective distance between grid node "*j*" and the neighboring point "*i*";

$\widehat{\boldsymbol{C}}_{\boldsymbol{j}}$ are the interpolated values for lattice node "*j*";

C_i are the neighboring points;

d_{ij} is the distance between grid node "*j*" and the neighboring point "*i*";

β is the Power or weighting parameter; and

δ is the Smooth parameter.

1. **Davis, John C. (1986) *Statistics and Data Analysis in Geology.* John Wiley and Sons, New York, NY.**
2. **Franke, R. (1982) *Scattered Data Interpolation: Test of Some Methods*, Mathematics of Computations, v. 33, n. 157, p. 181-200.**

3D nano-scanner/Imager

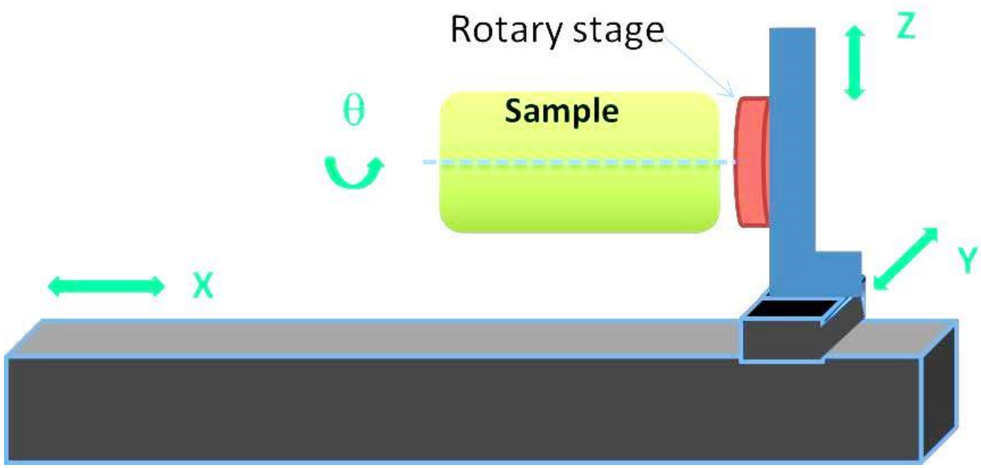

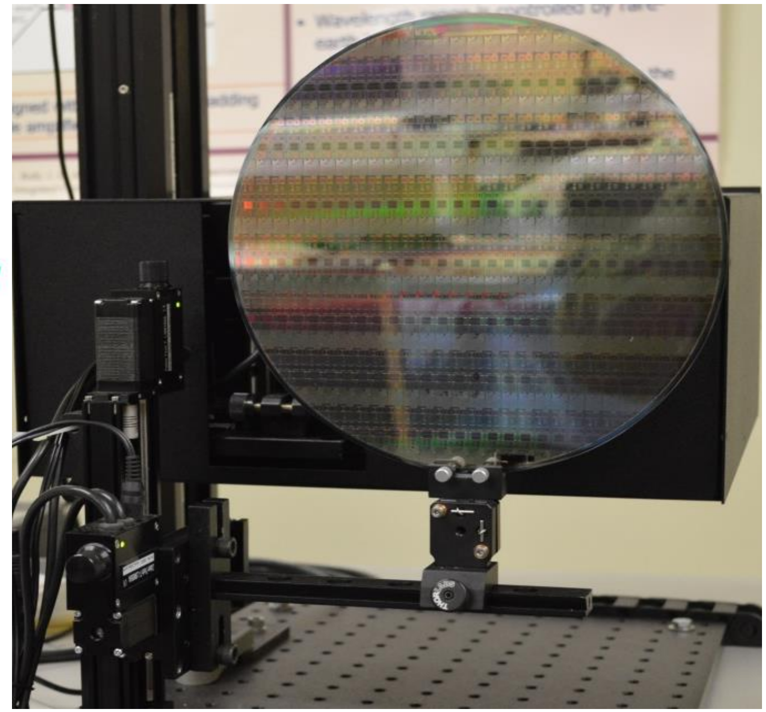

Scan X, XY, or XYZ for profiling and/or reconstructed imaging
Angular scan for conformal imaging

A test wafer is mounted on the nanoscanner.

Reproducibility

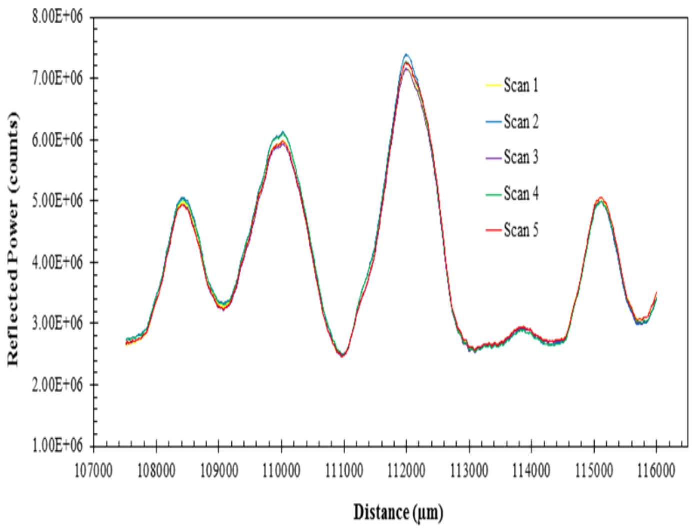

Reproducibility of the traces. Very slight mismatch is due to the course resolution of the stage. This will improve by installing a higher resolution stage.

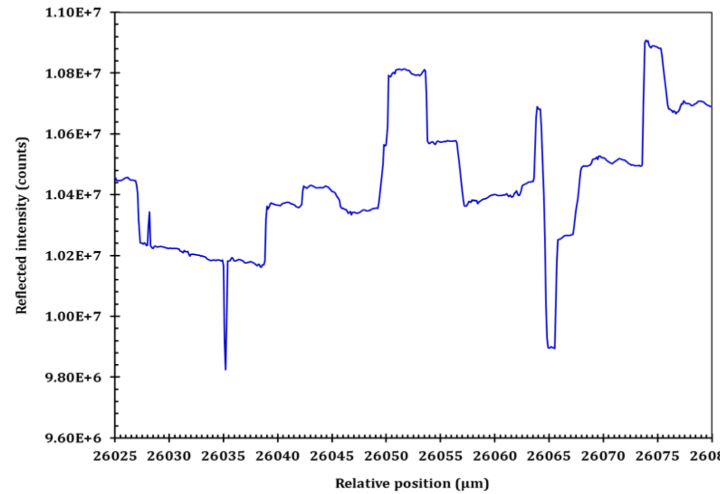

changes in reflectivity based on material on wafer

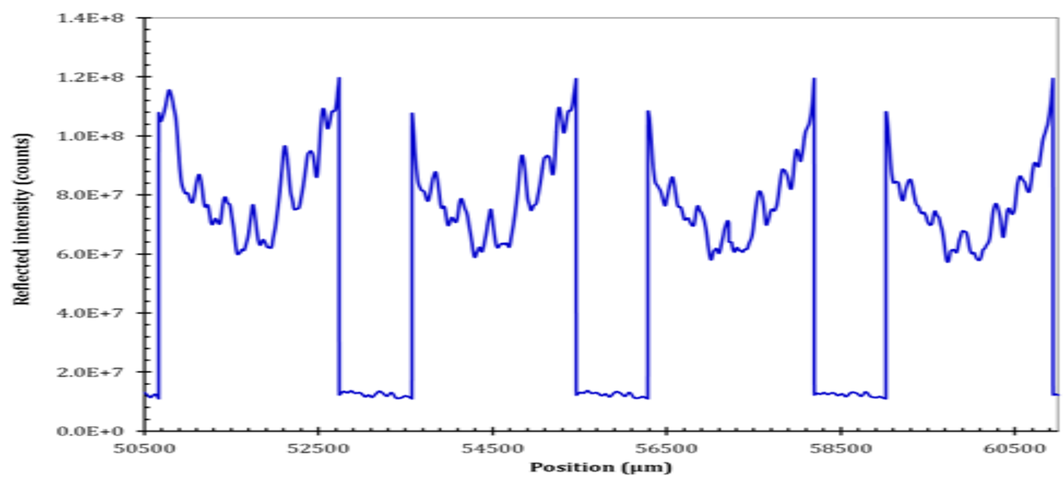

high resolution scan revealing periodic pattern from adjacent segments of a wafer

Example: Cr3 on glass slide

Structure of 1 cubic micron

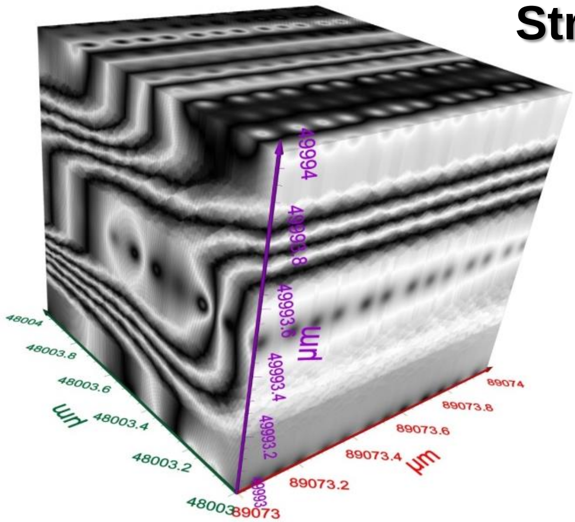

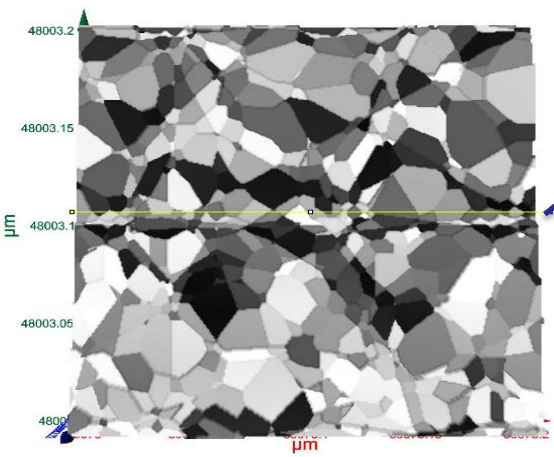

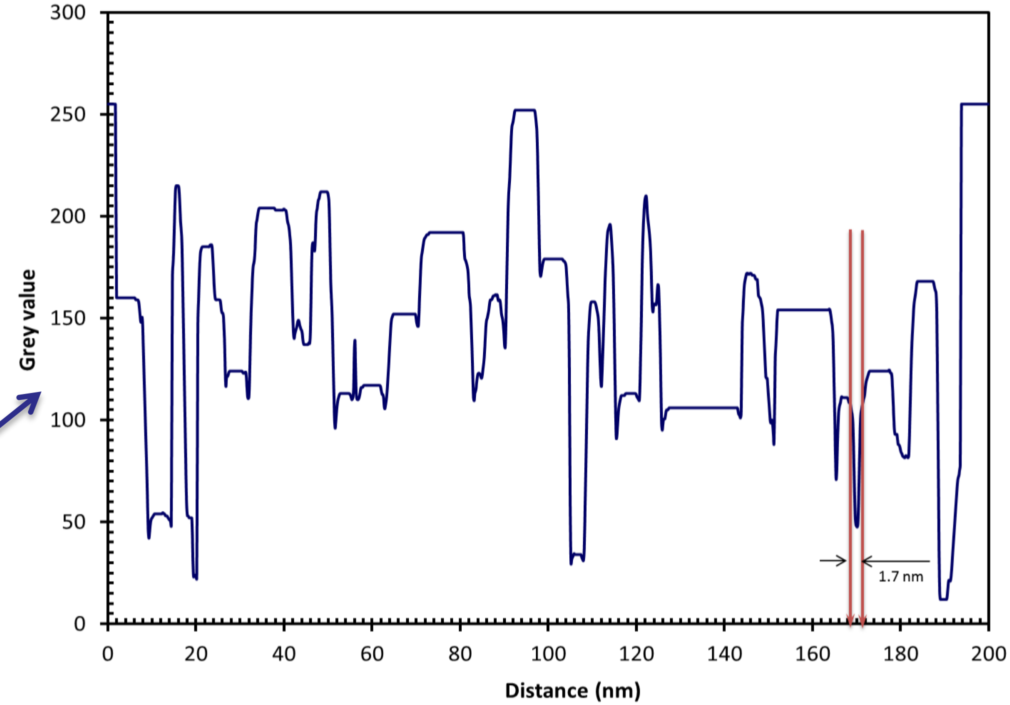

200 nm x 200 nm close-up of a surface

Analysis along the yellow line shows the smallest particle size ~ 1.7 nm.

High Resolution Analysis

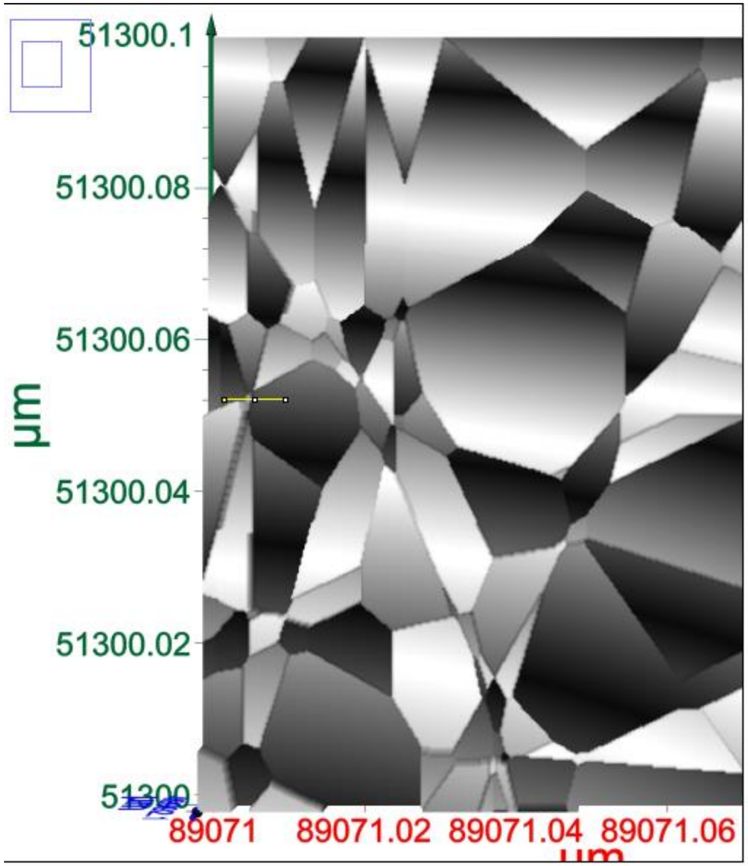

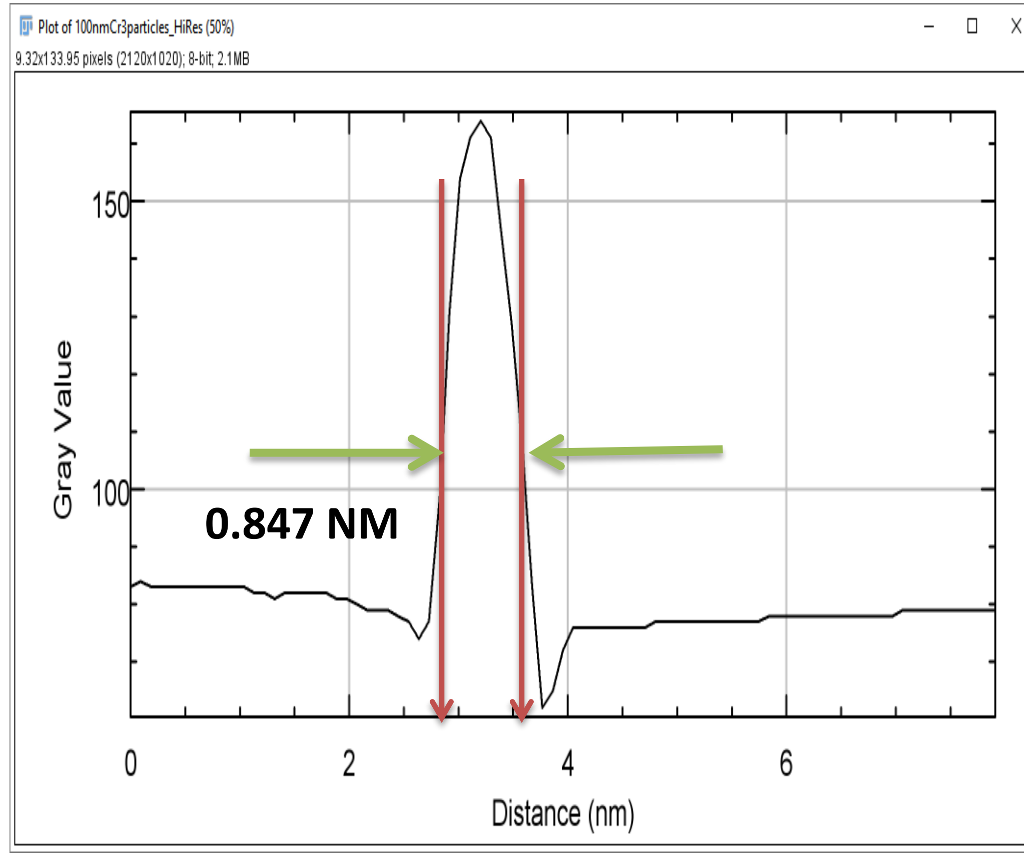

Cr3 nanoparticles on glass slide. Smallest particle detected is ~8.5Å (<1 nm).

Terahertz imaging of stratum corneum

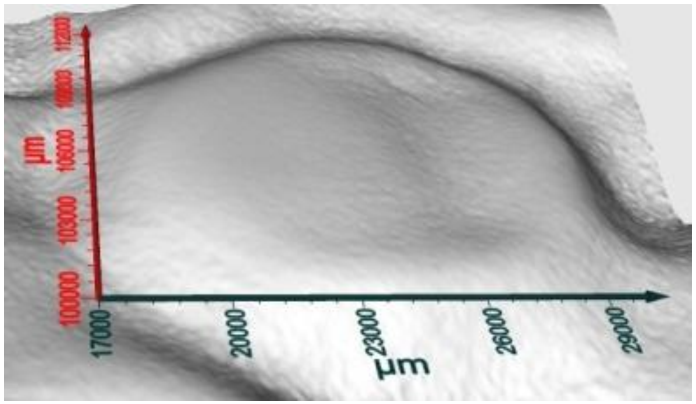

Reconstructive image of a piece of human stratum corneum

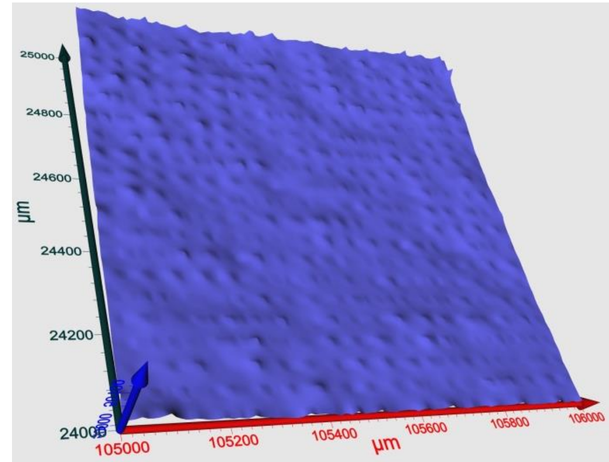

Closeup of 1 mm x 1 mm area. Small features visible

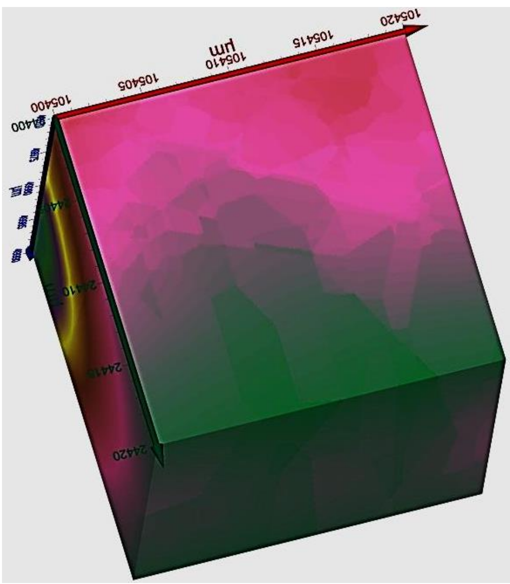

3D image of 20 micron cube

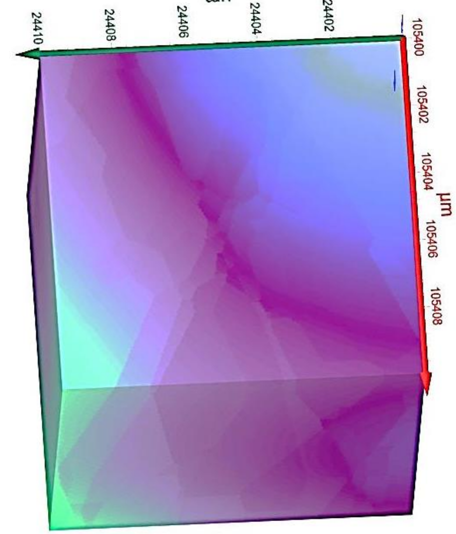

3D image of 10 micron cube

Image comparison

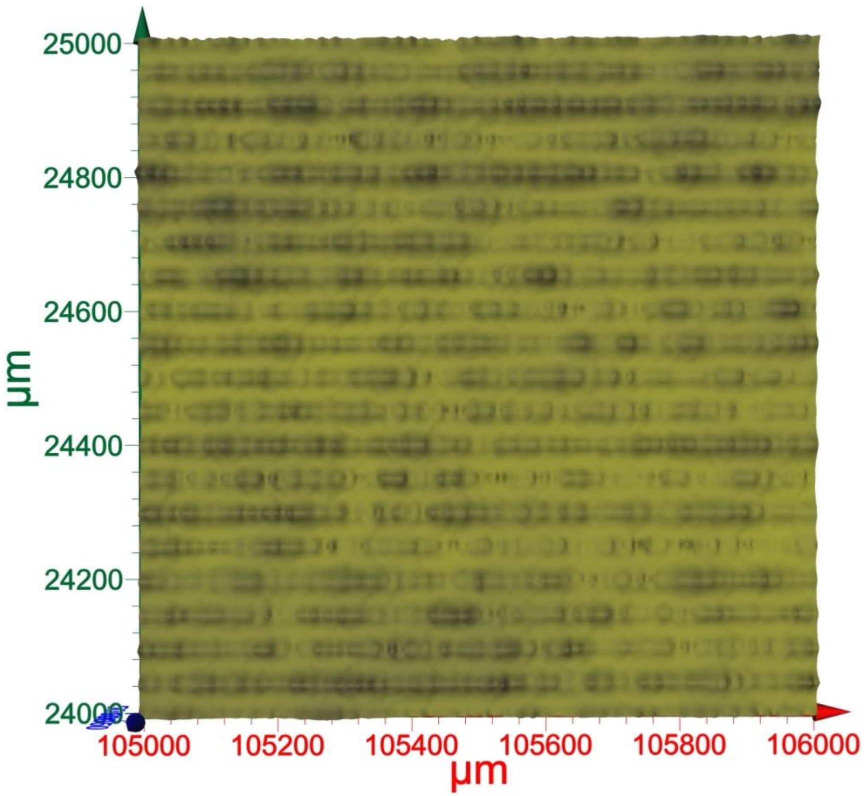

1 mm² stratum corneum alone.

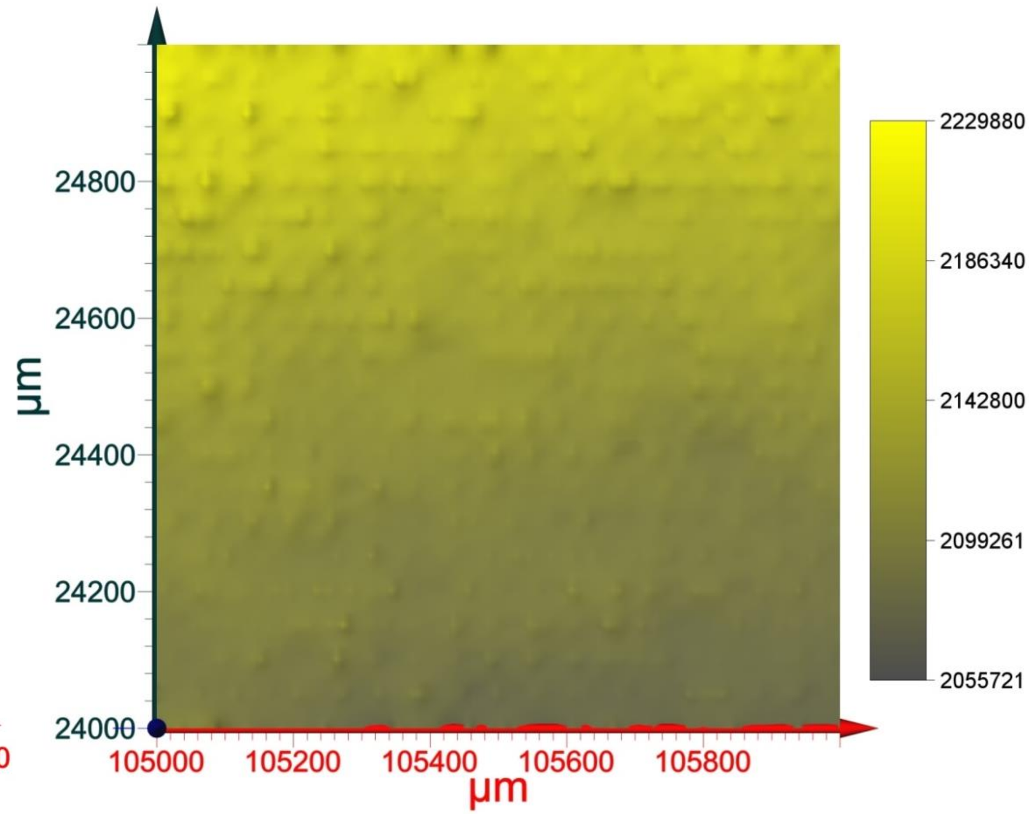

1 mm² stratum corneum after Cr3 permeation. Higher reflection

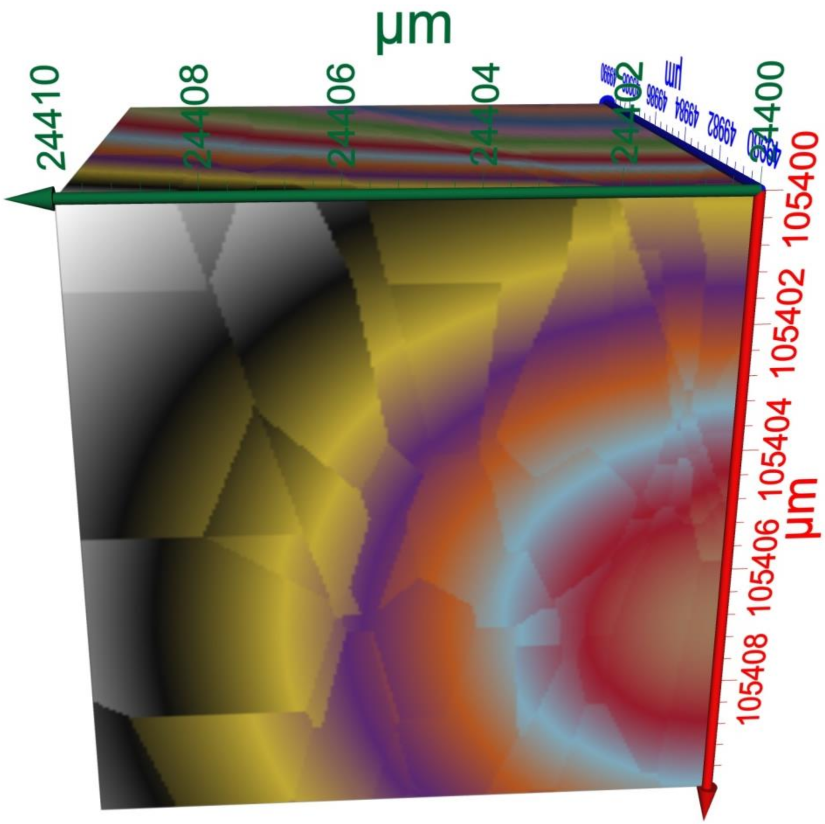

No Cr3, 10 cubic micron

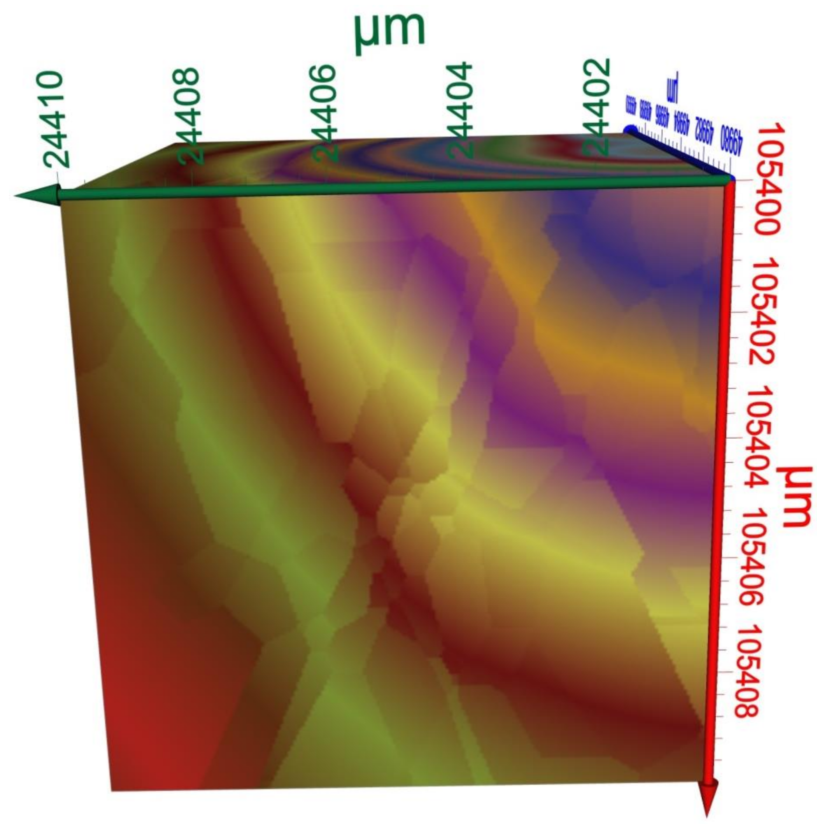

After Cr3 permeation, 10 cubic micron

Image comparison

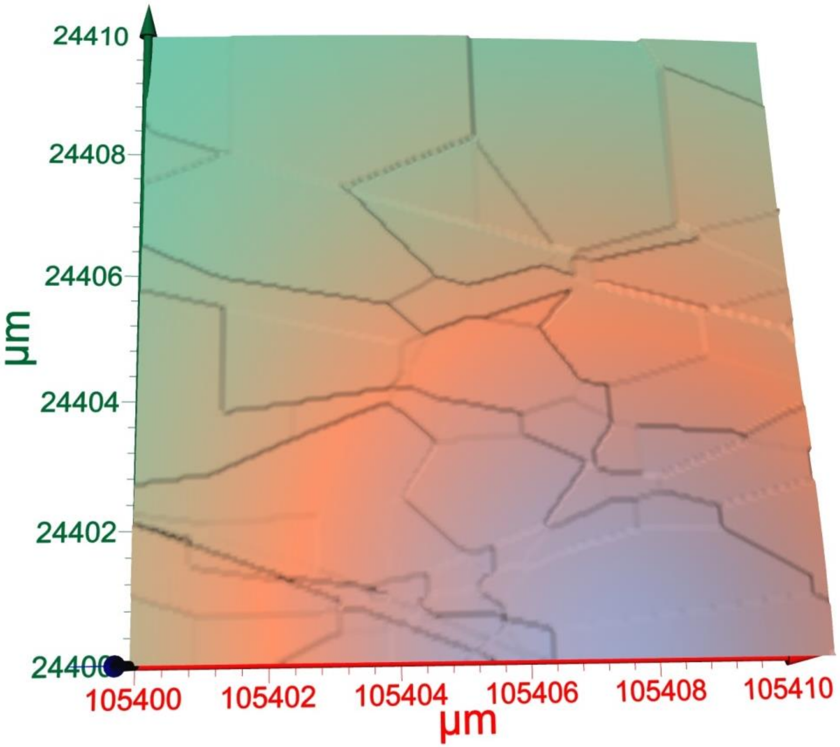

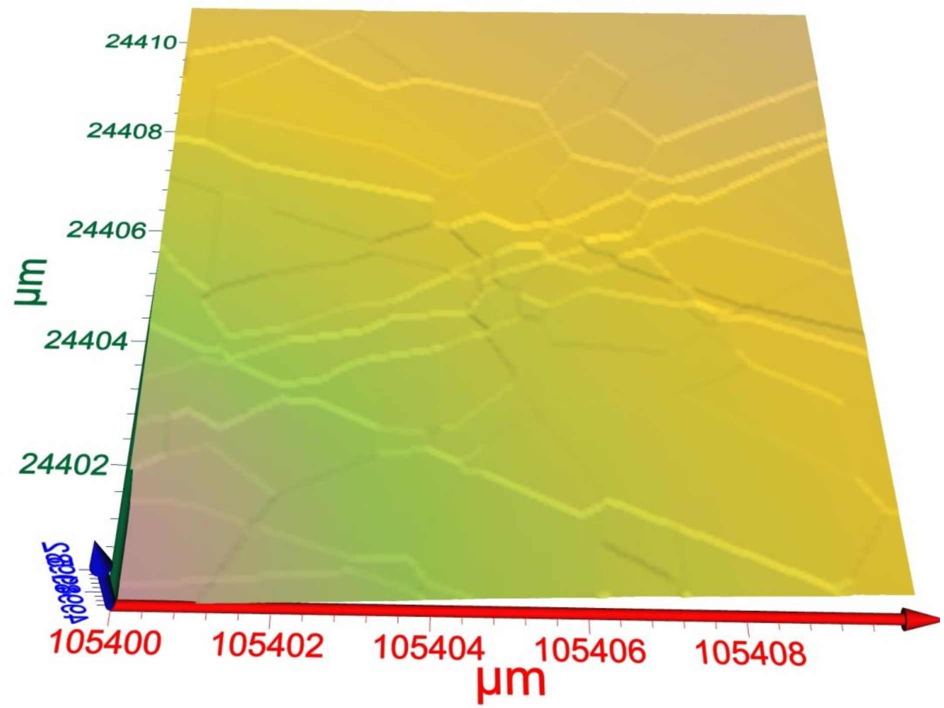

10 µm^2 stratum corneum alone
Boundaries are well defined

10 µm^2 stratum corneum after Cr3 permeation. Boundaries are less prominent

3D image of skin

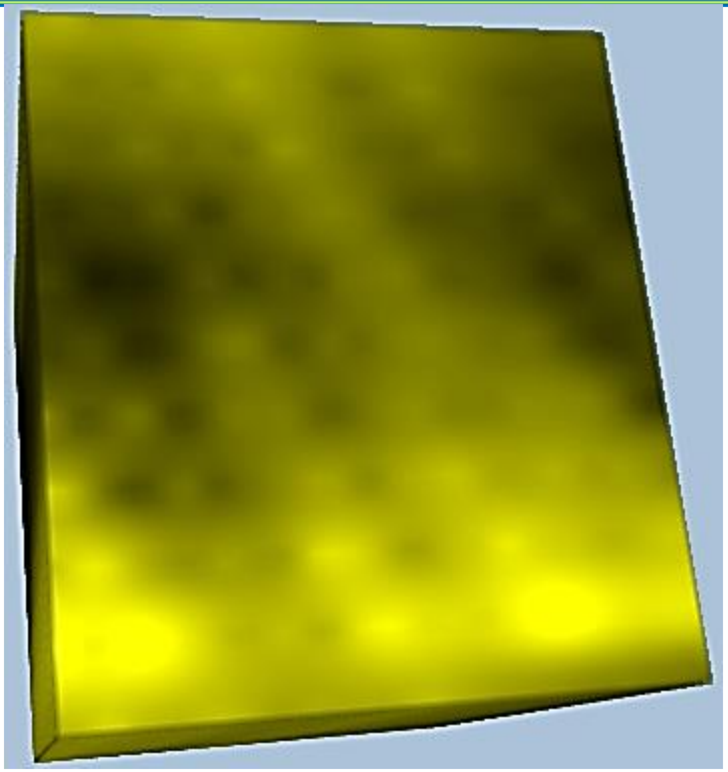
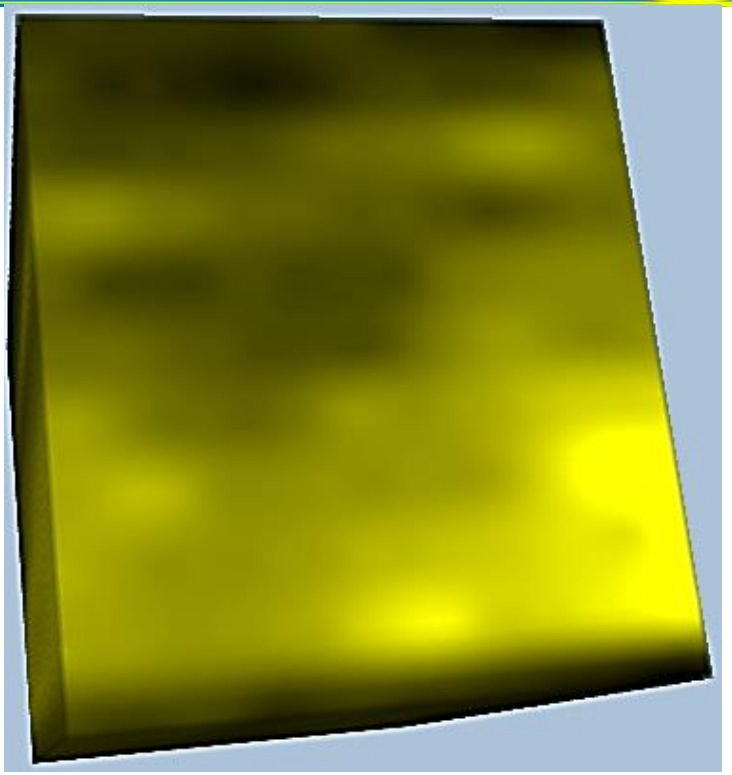

Reconstructed 3D image of healthy skin (left) and skin with basal cell carcinoma. Healthy sample was scanned over 1 mm × 1 mm × 1.2 mm and BCC sample was scanned over 1 mm ×1 mm × 1.5 mm. The top surface of healthy skin shows regular cell pattern (left) while the BCC samples has lost regular cell patterns and exhibit more agglomerated structure.

Layer by layer image

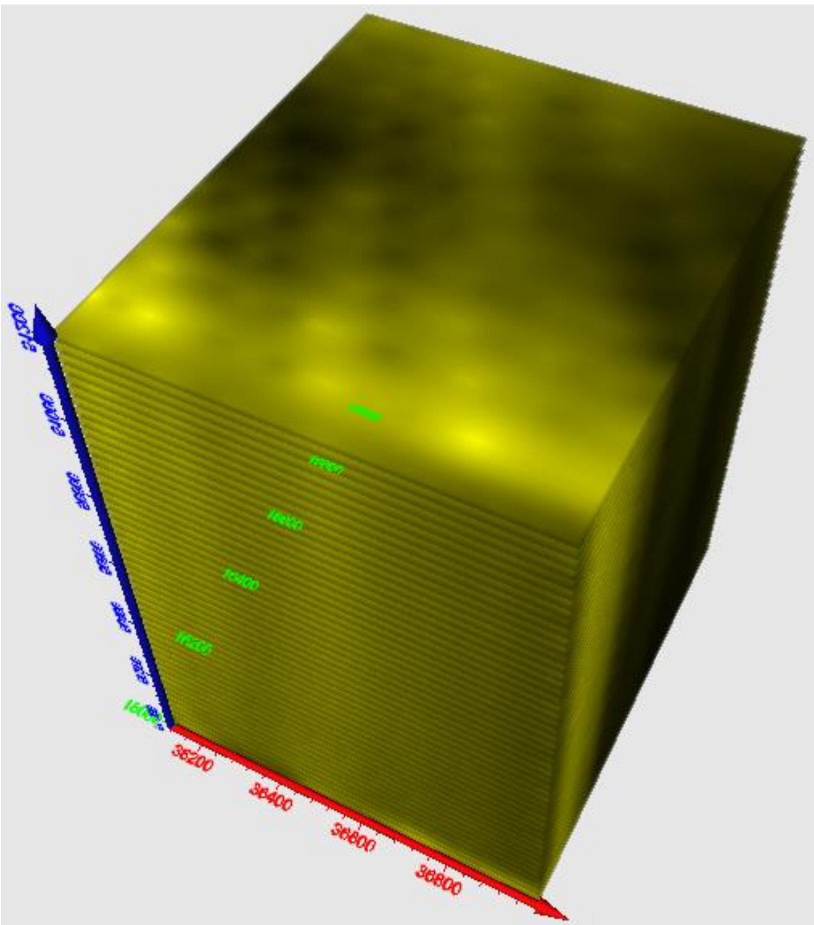

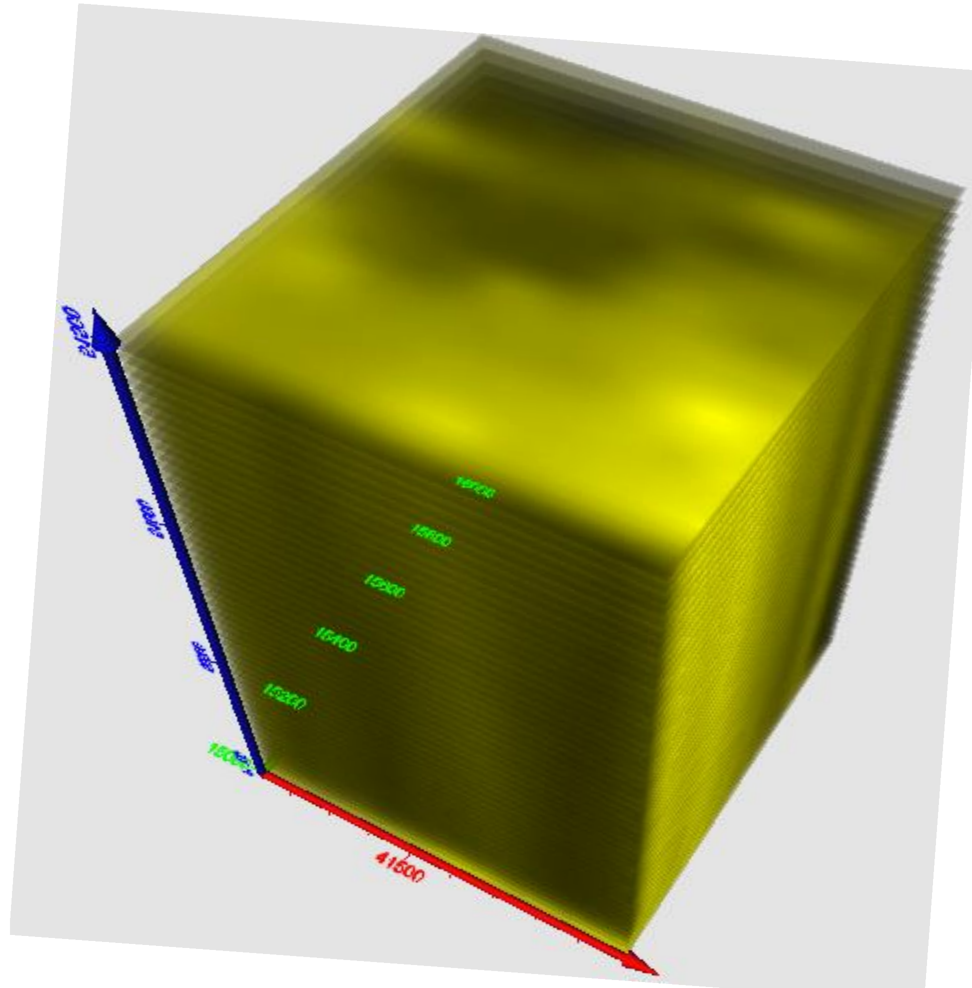

Benign

Basal cell carcinoma

3D image analysis

Skin Type	Normal	Lentigo	SCC
3D Image analysis	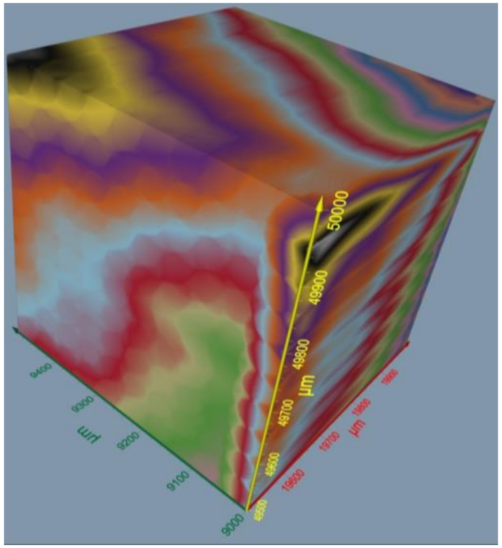 Normal skin shows regular cell pattern and layered structure.	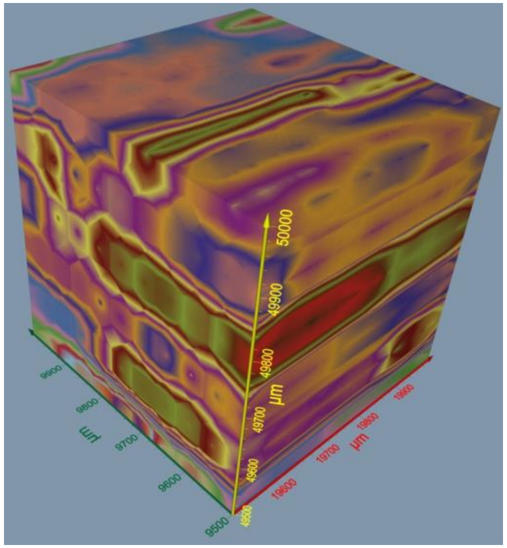 Lentigo skin does not show regular cell pattern. The layering seems patchy and different than normal skin.	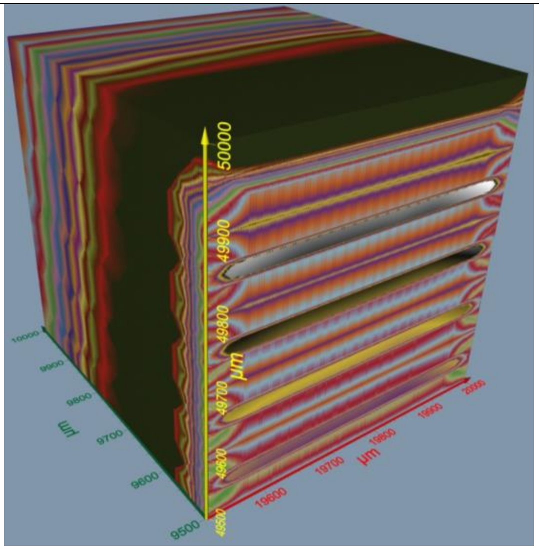 SCC skin also has no regular cell pattern. The layering structure is also quite different than both the normal and Lentigo skins.

Image comparison of different skin conditions

Skin Type	Front	Bottom	Left	Right-2
Normal	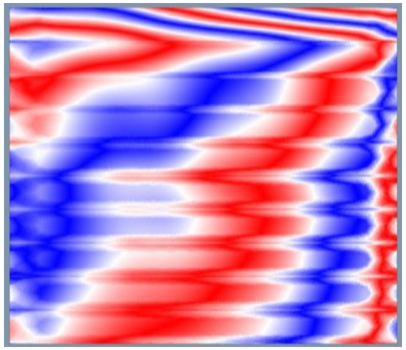	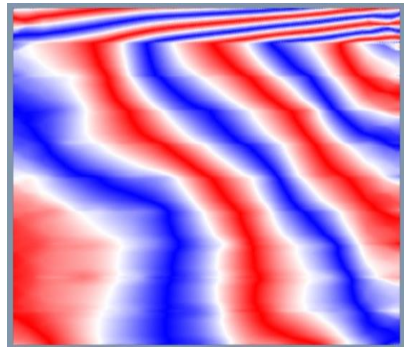	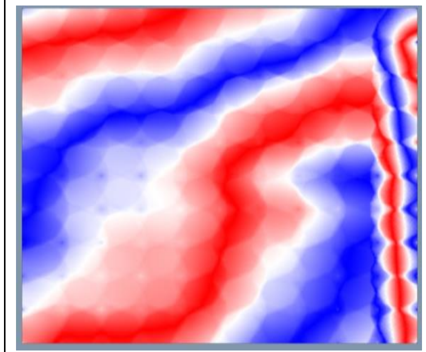	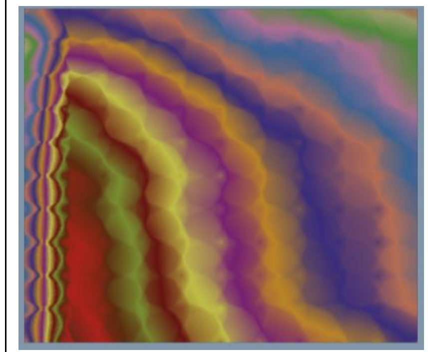
Lentigo	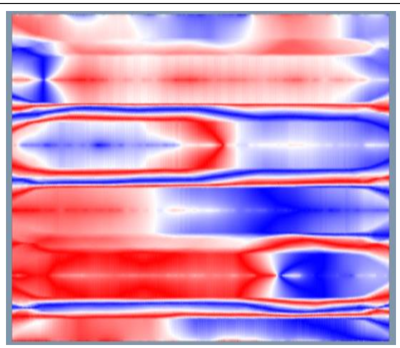	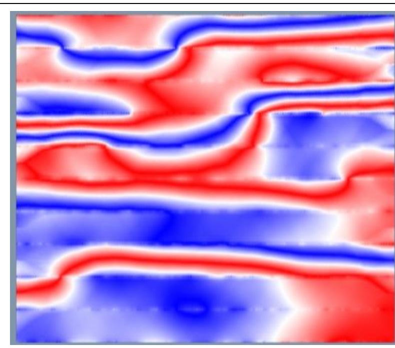	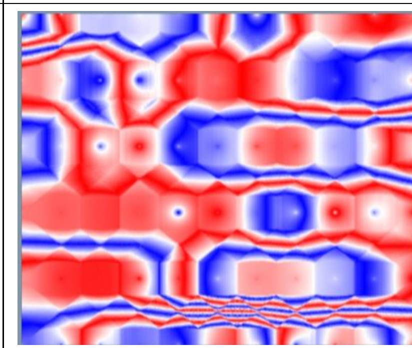	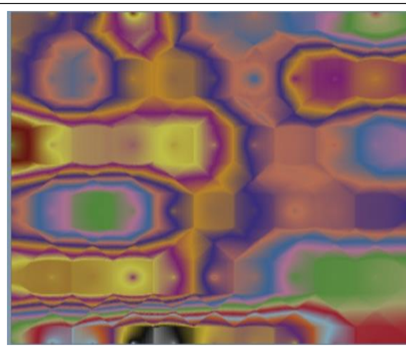
SCC	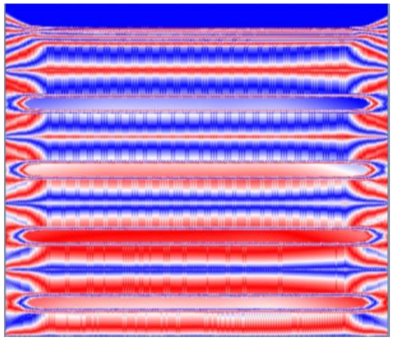	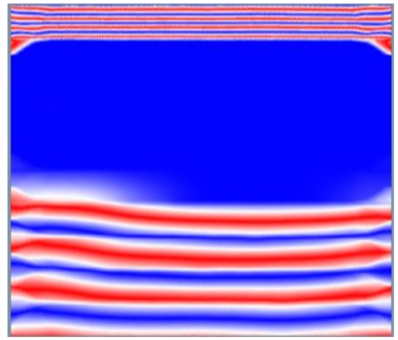	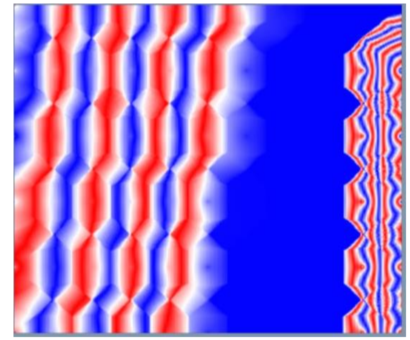	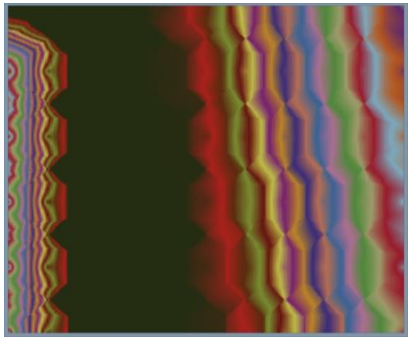

Single cell analysis

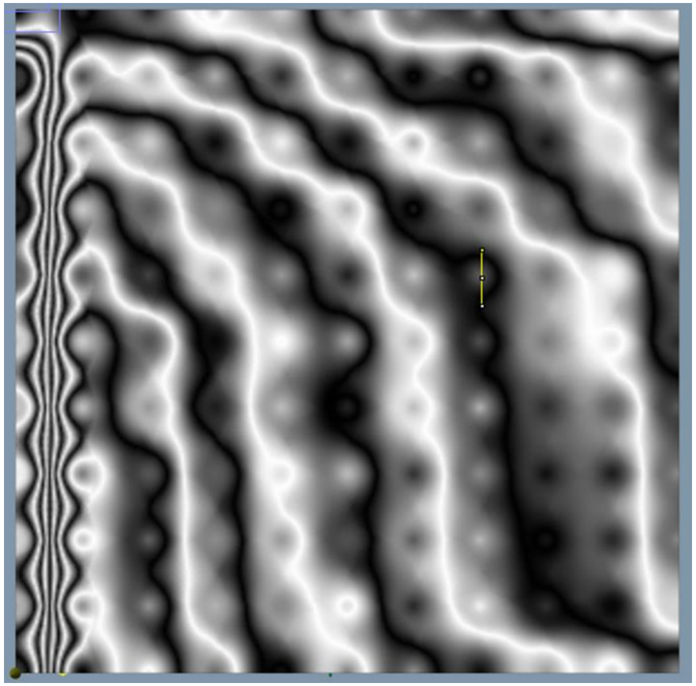

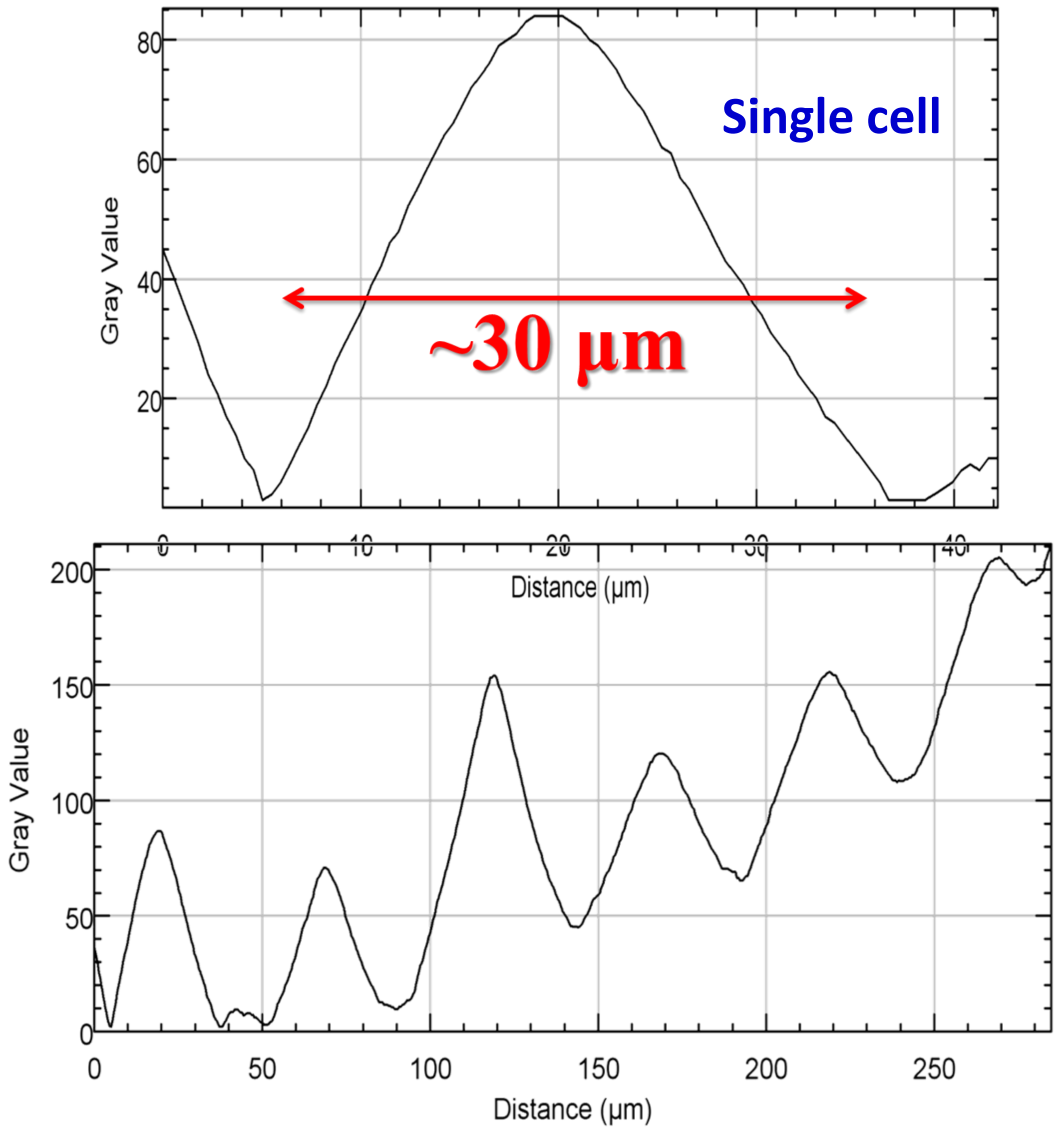

Multiple cells →

Isosurface analysis

Skin Type	Normal	Lentigo	SCC
Isosurface Image analysis	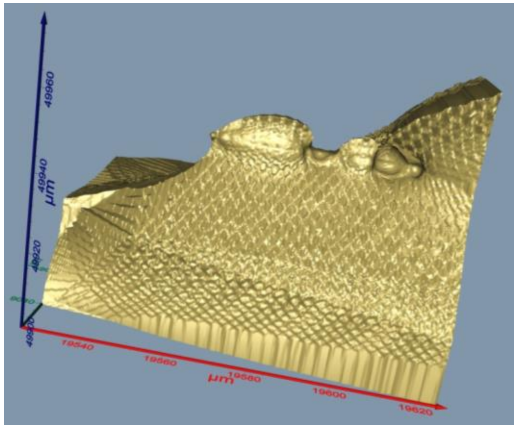 Normal skin shows regular cell pattern; different structural features are visible.	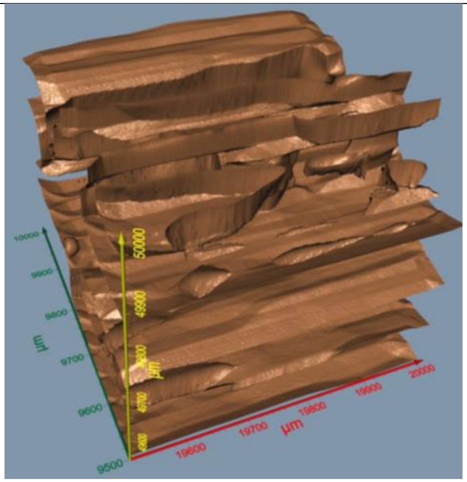 Lentigo skin does not show regular cell pattern. The layering seems patchy and different than normal skin.	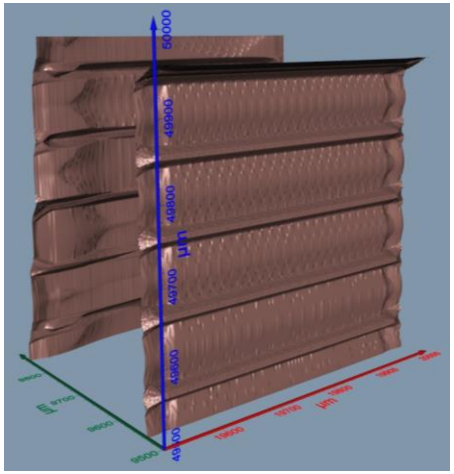 Regular cell pattern totally deteriorated for SCC skin. The layering structure is also vanished.

Layer by Layer visualization

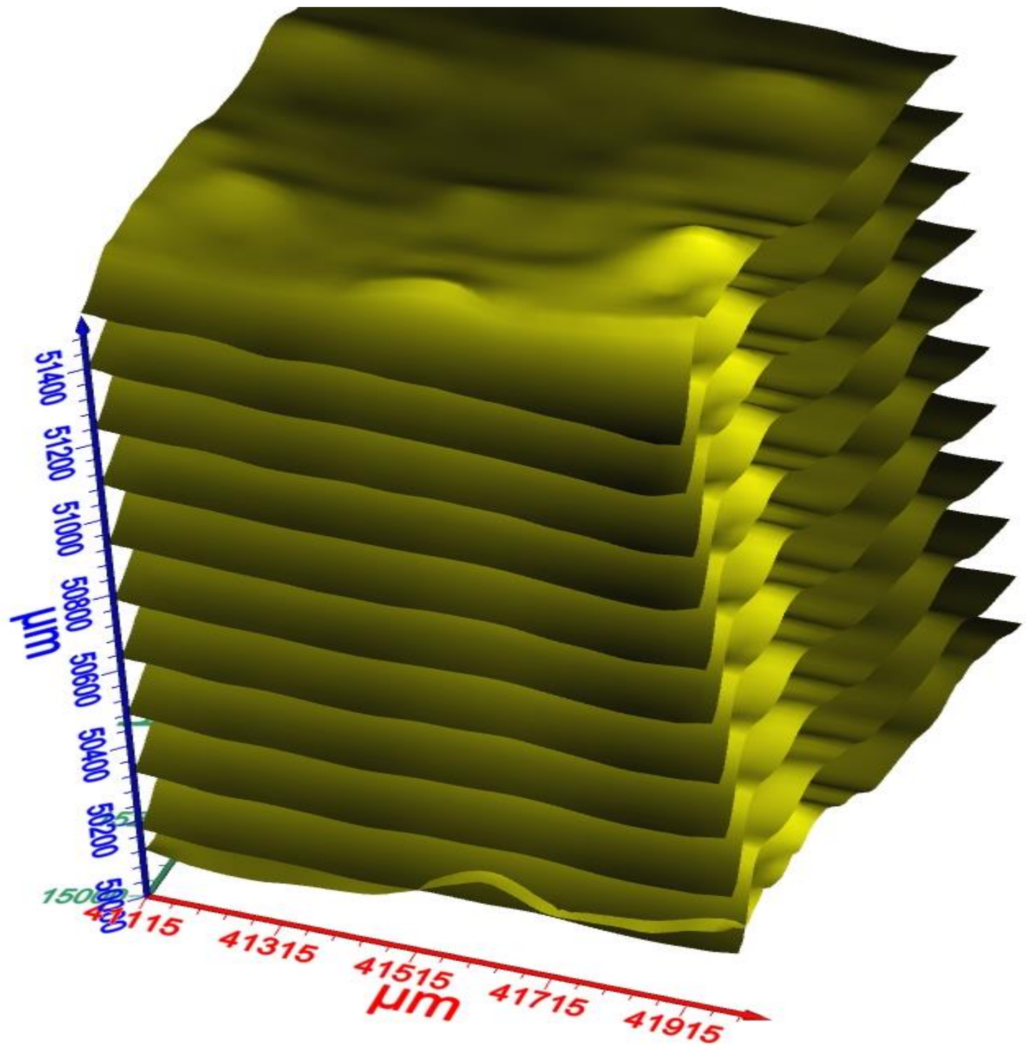

Layer by layer image

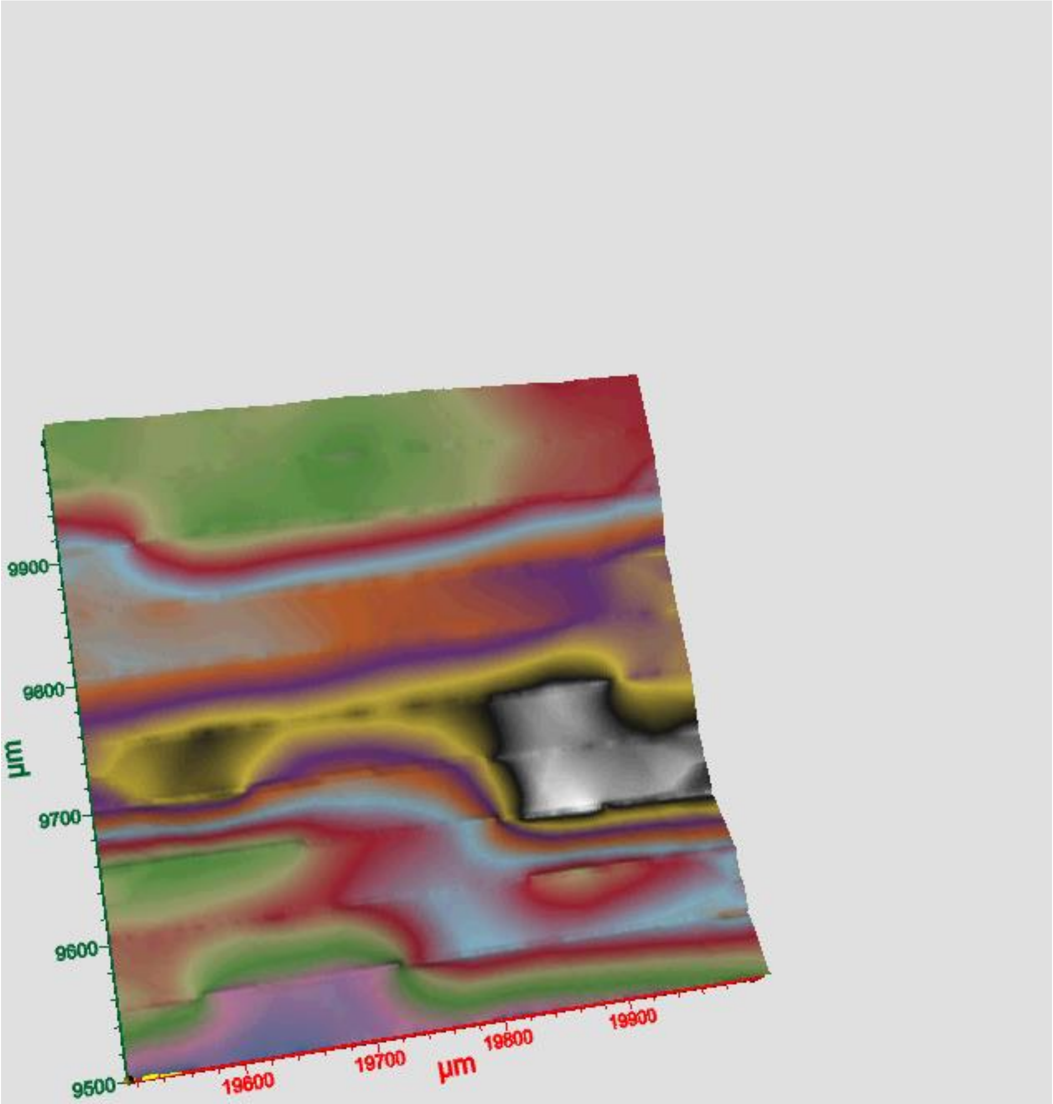

Thickness profile

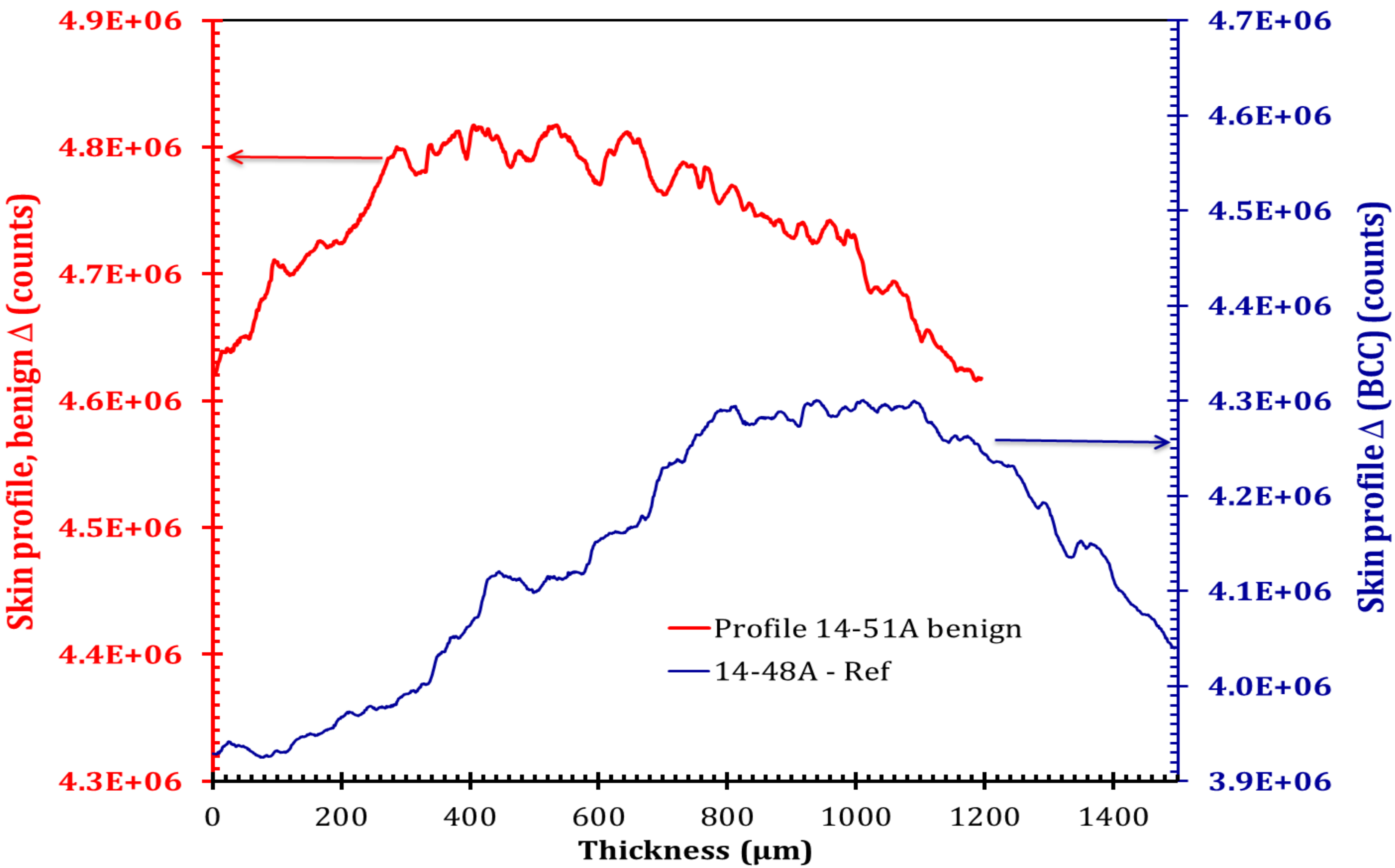

Diffusion kinetics

- Fick's first law:

$$J = -D\frac{\partial C}{\partial x}$$

C is the concentration and

D is the diffusion coefficient

- Fick's second law:

$$\partial C/\partial t = D\frac{\partial^2 C}{\partial x^2}$$

Permeation Kinetics

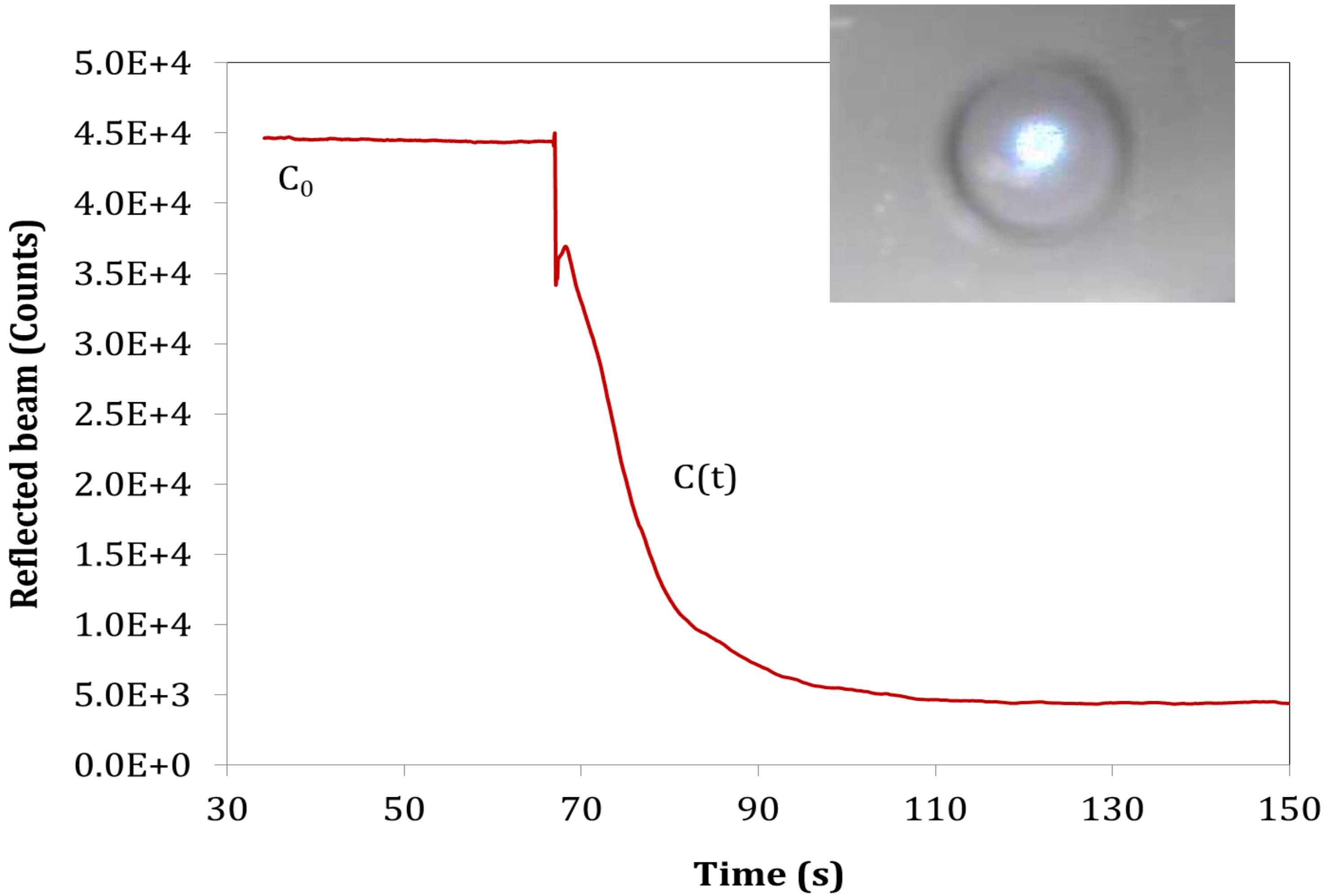

Example: Permeation kinetics of DI water in glossy paper

Concentration gradient

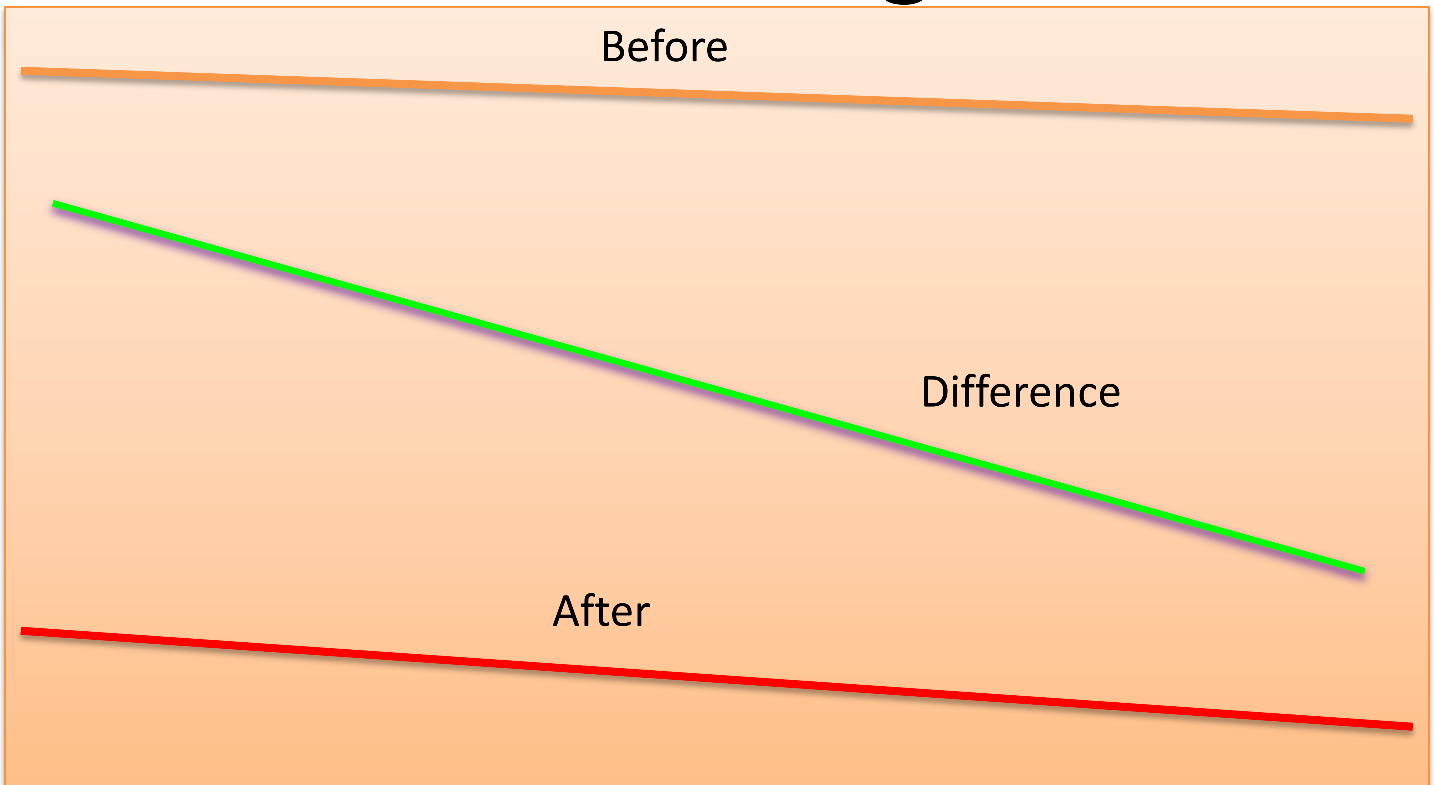

$$\left|\frac{\partial C}{\partial x}\right|_{Analyle} = \left|\left|\frac{\partial C}{\partial x}\right|_{Before} - \left|\frac{\partial C}{\partial x}\right|_{After}\right|$$

Hydrocortisone Kinetics

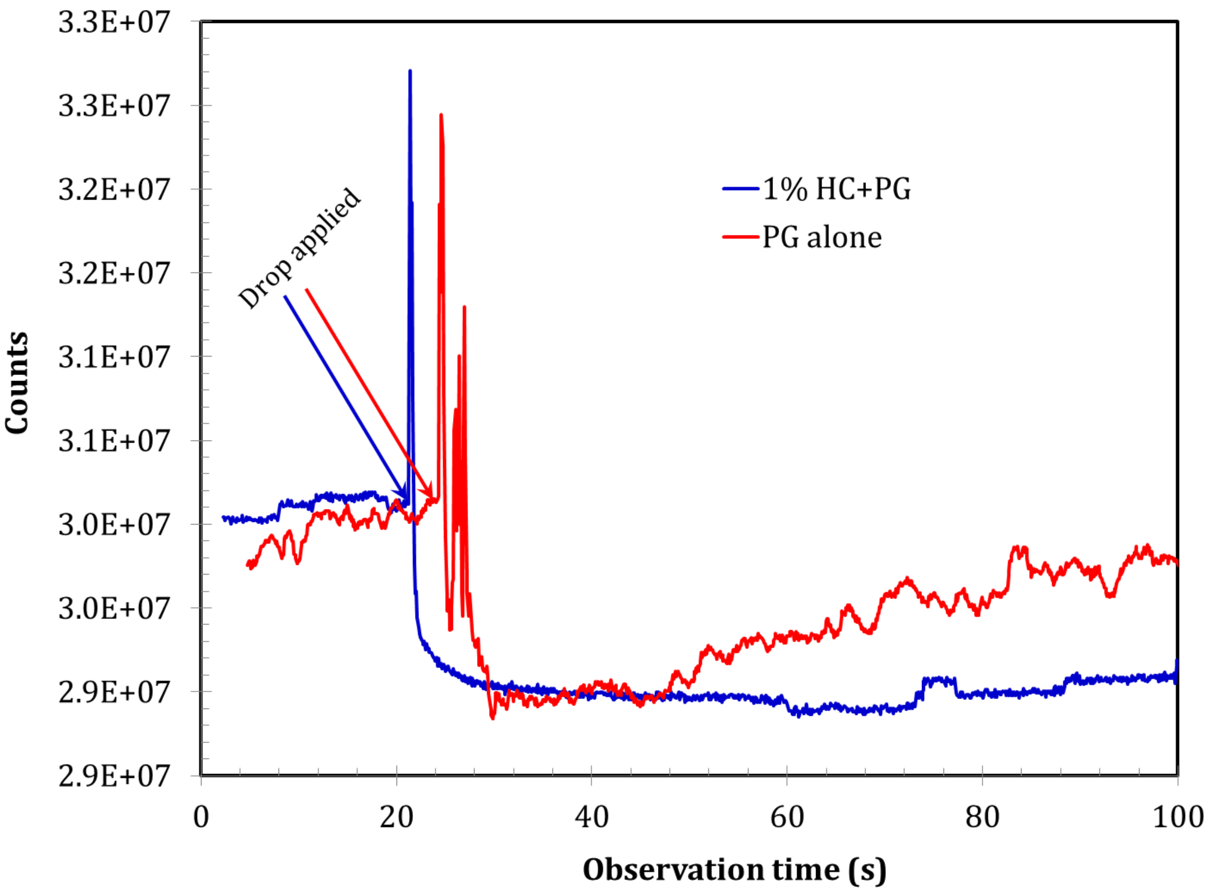

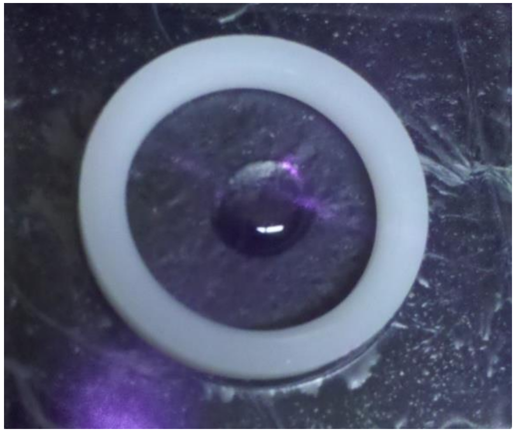

Stratum Corneum mounted on the sample holder

Kinetics of permeation of two solutions in to stratum corneum:

Red: Propylene glycol

Blue: 1% hydrocortisone in propylene glycol

Concentration gradient of Hydrocortisone

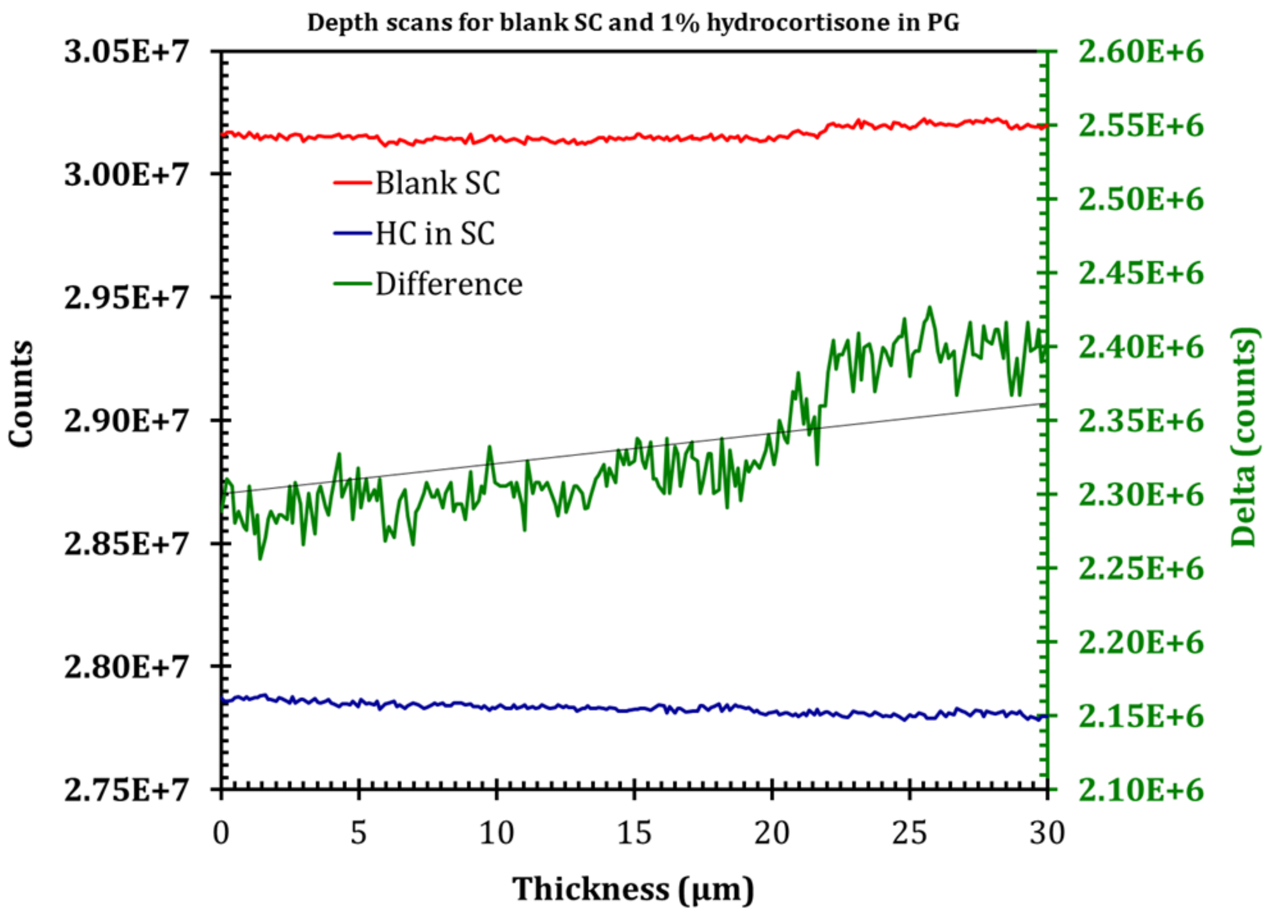

Semiconductor imaging

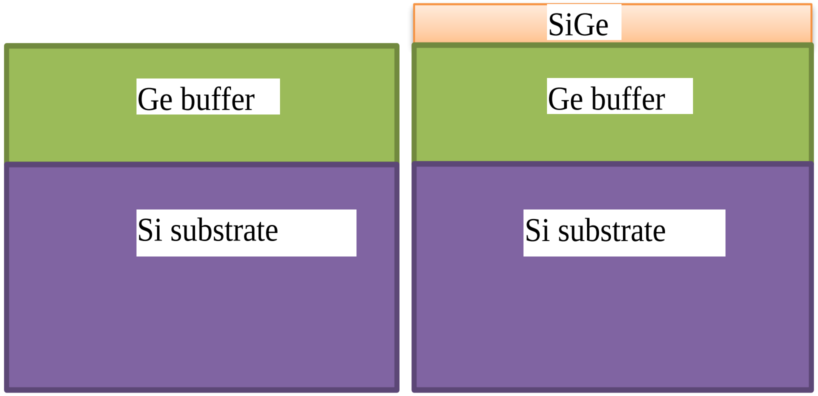

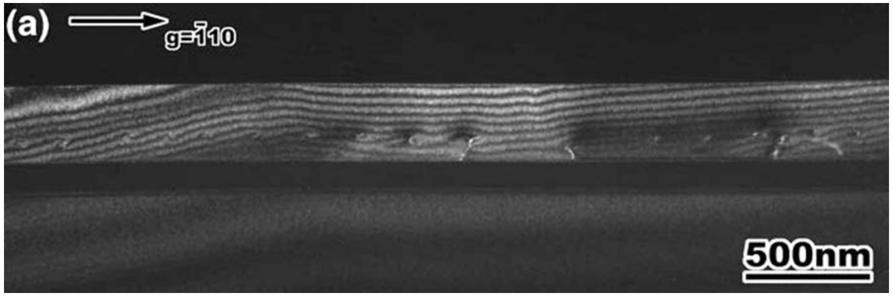

Stacking fault in SiGe layer [11]

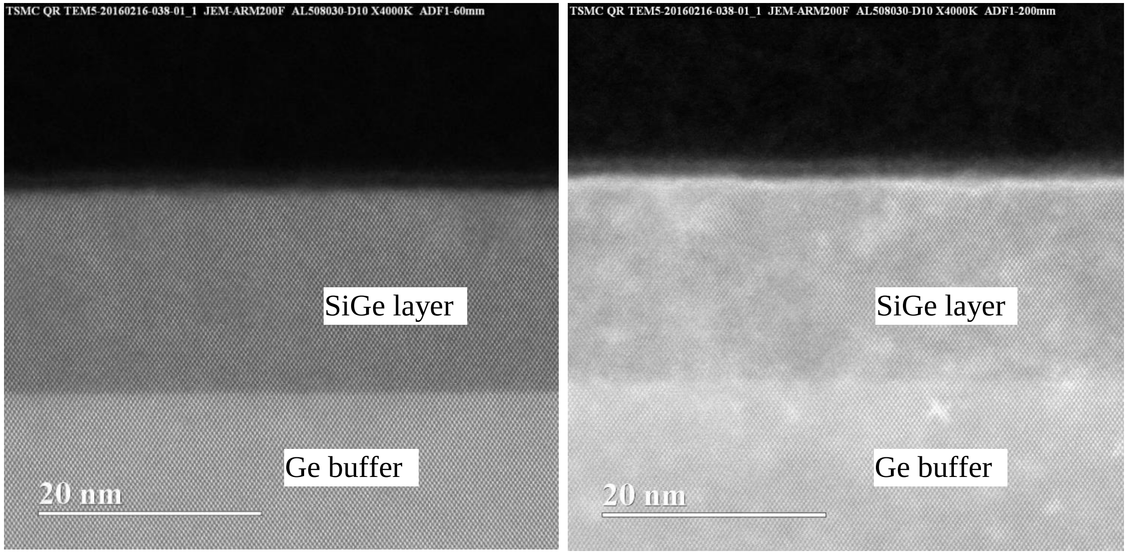

TEM image of actual sample

Stacking fault

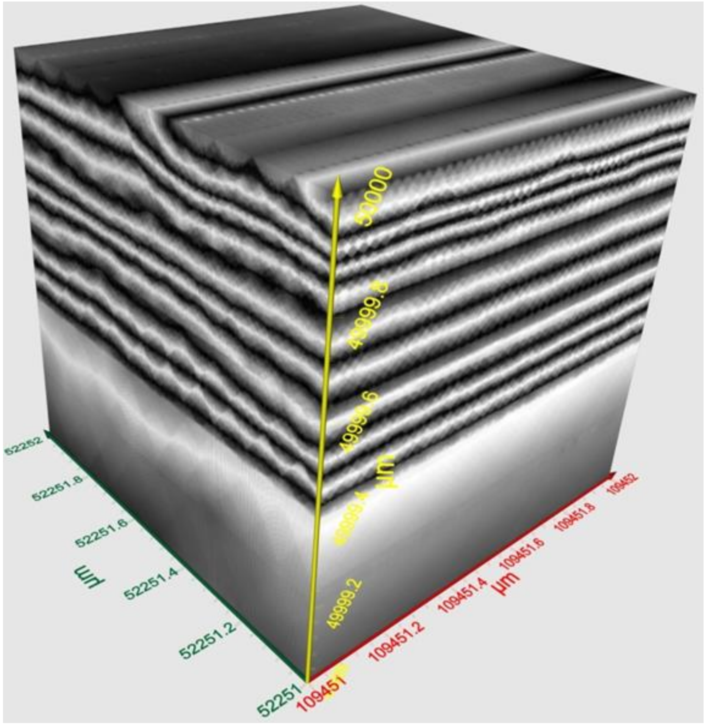

1 µm³ volume of D02

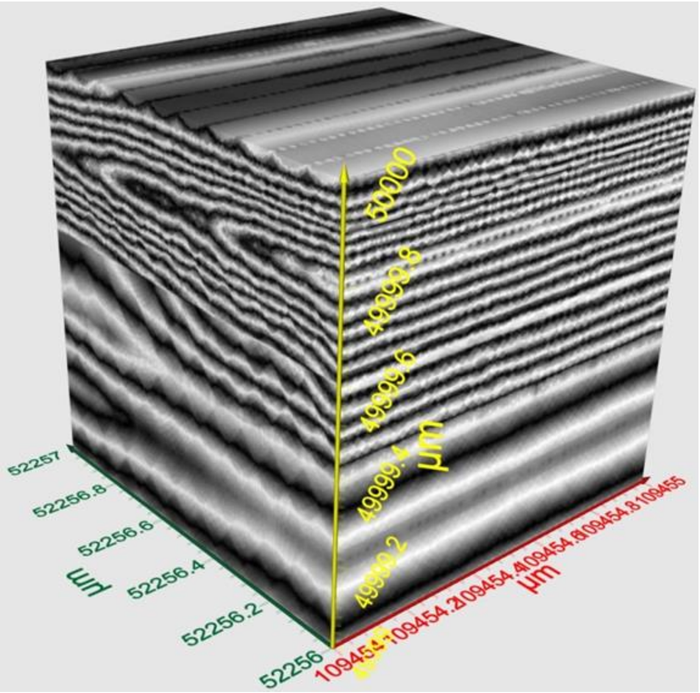

1 µm³ volume of D10

Layer thickness

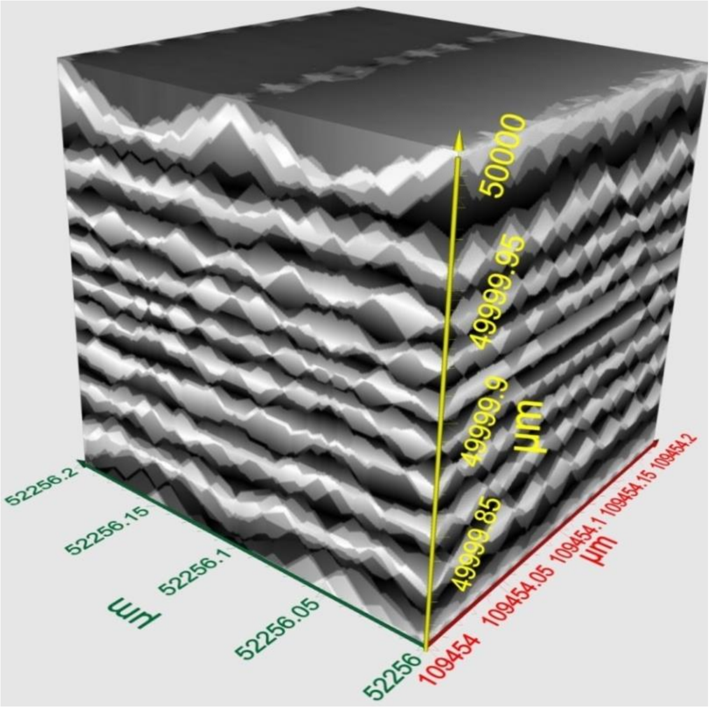

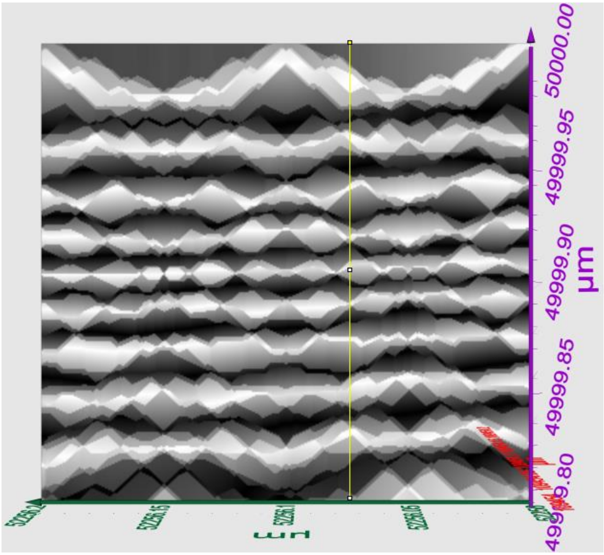

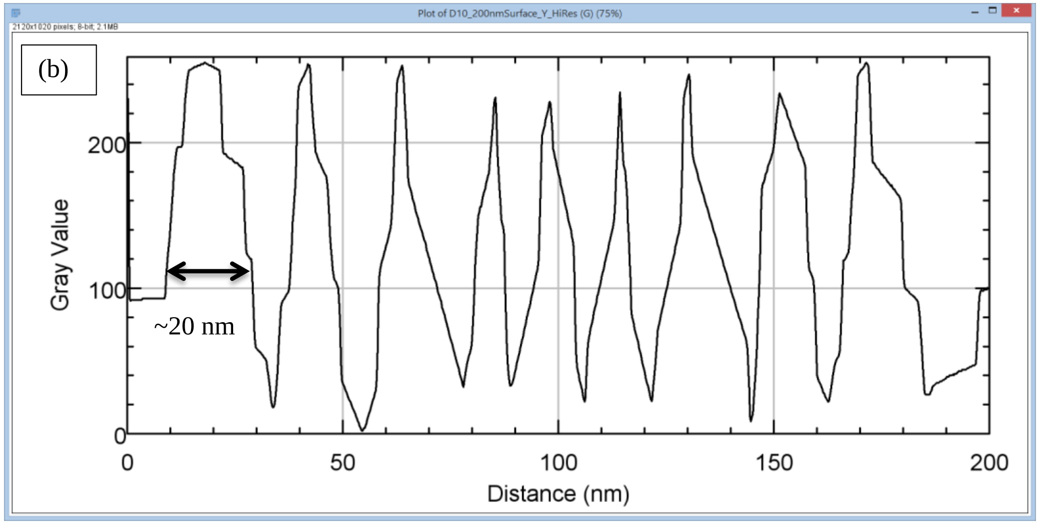

200 nm³ close-up of D10

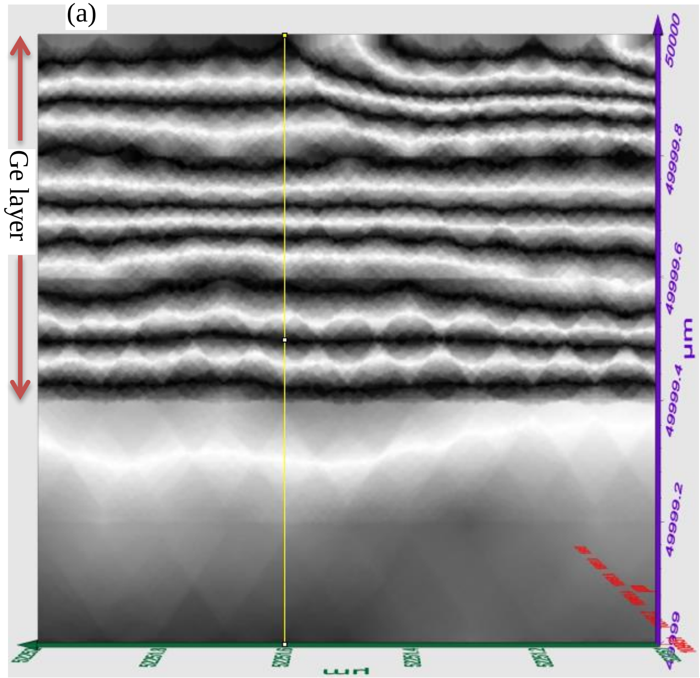

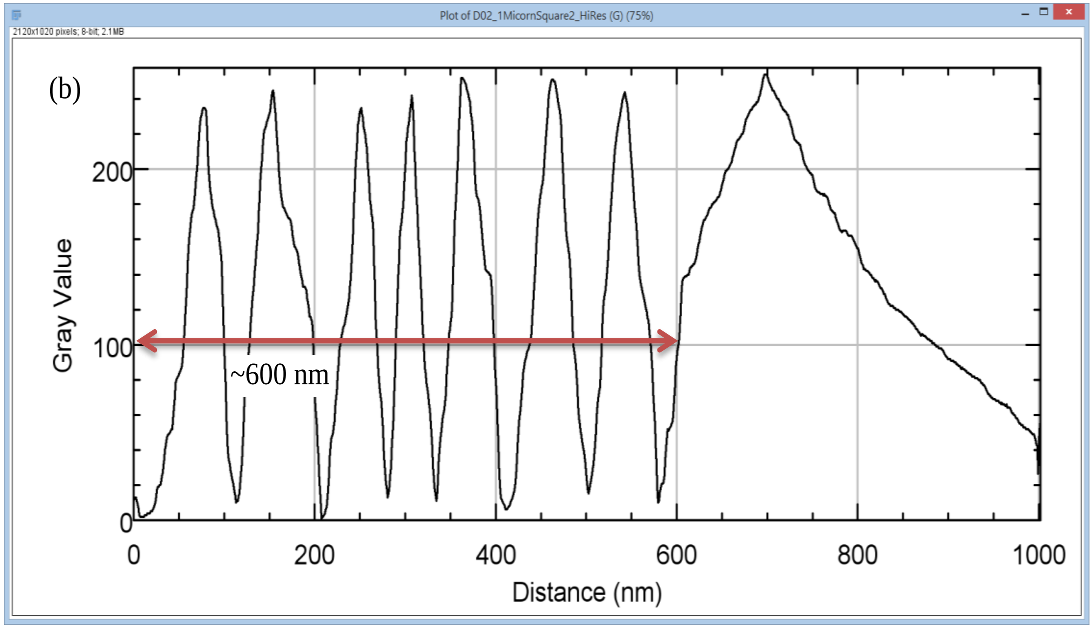

Vertical cross-section surface, 1 µm x 1 µm. (b) Analysis along the yellow line in (a) shows the top layer is ~ 600 nm. However, some non-uniformity is visible in the top layer thickness.

Quantum dot imaging

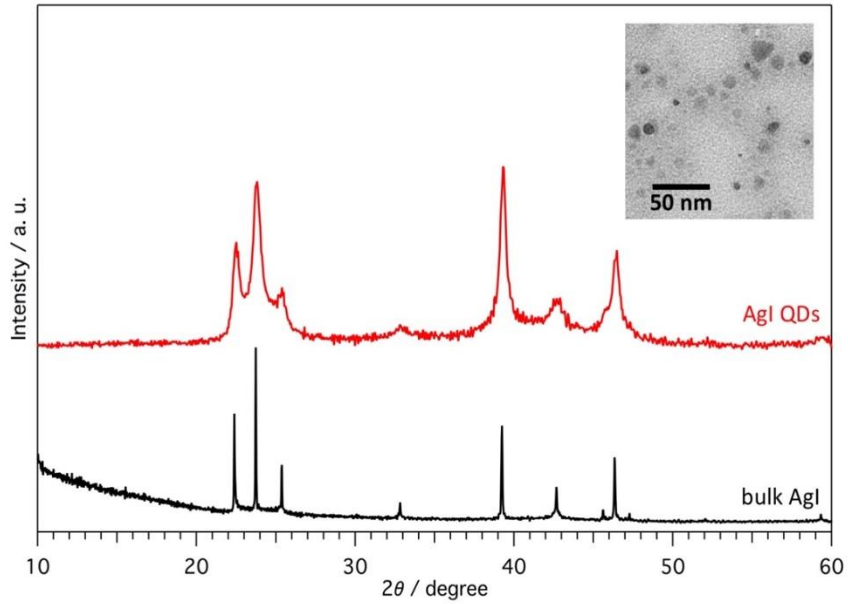

PXRD and TEM analysis shows the AgI quantum dots are ~(11 ± 4.5) nm.

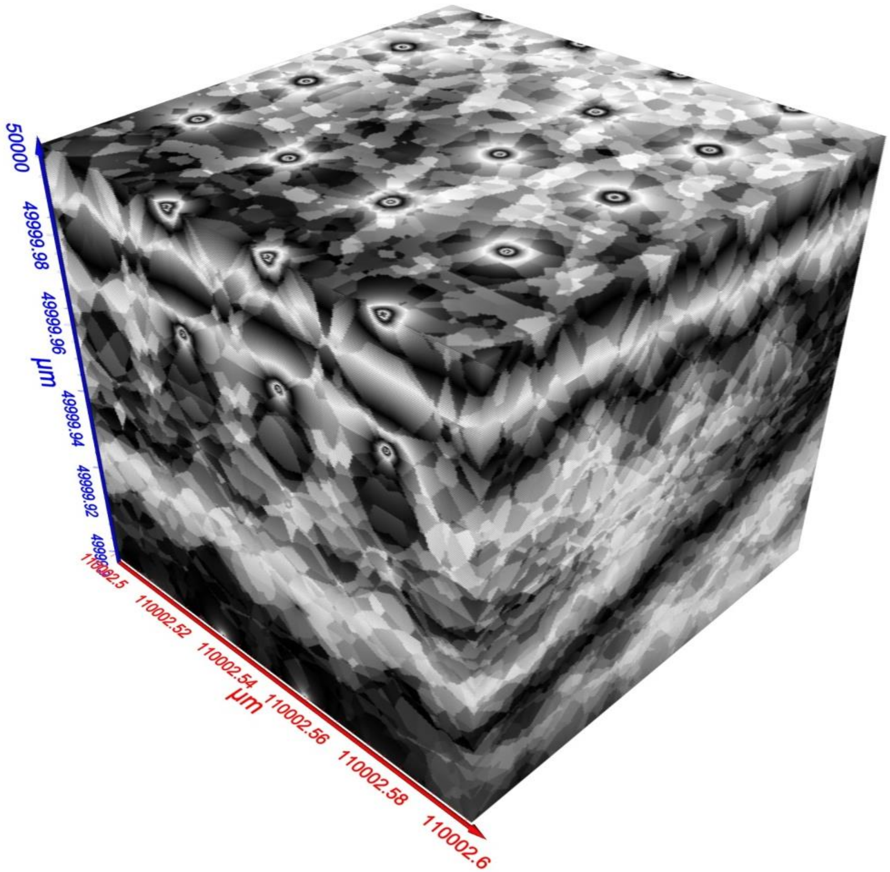

100 nm^3 volume (close up) extracted from the 5 µm^3 scanned volume.

QD size analysis

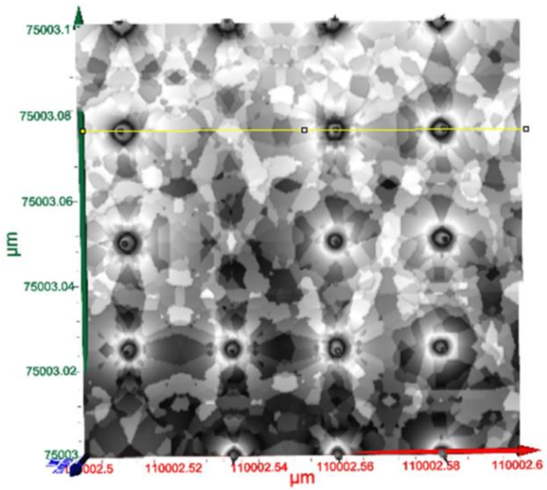

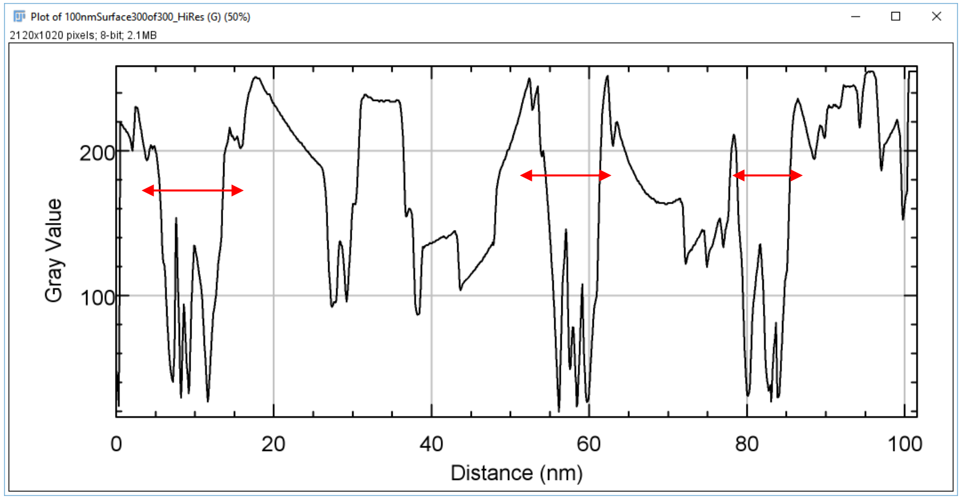

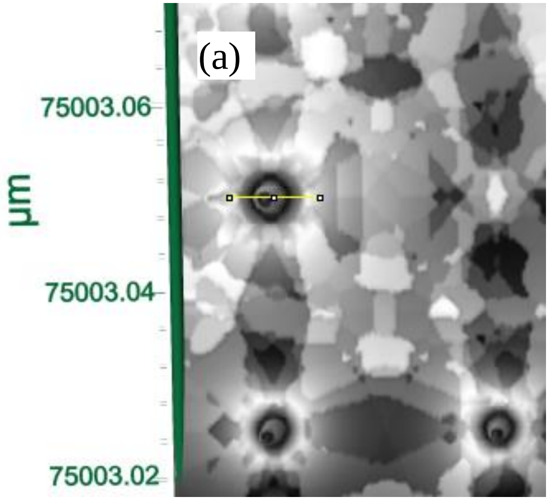

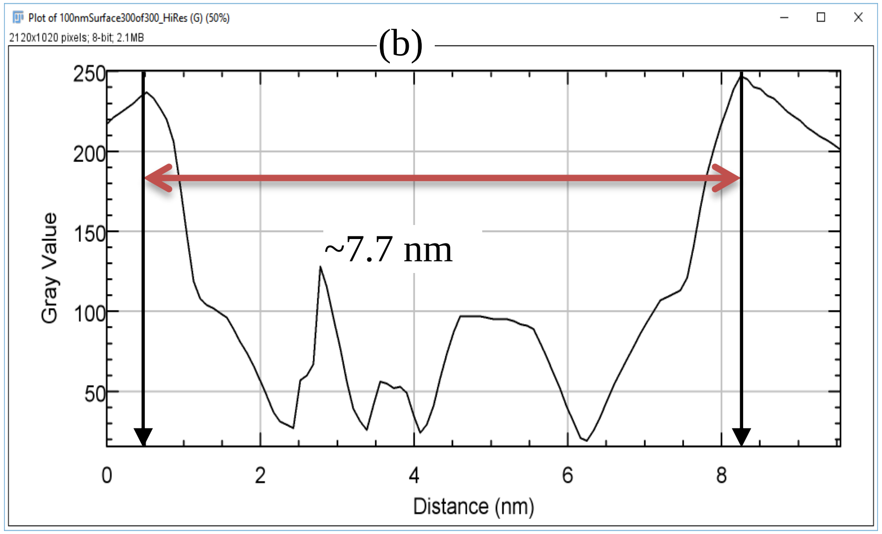

Conclusions

- Integrated Terahertz nanoscanning spectrometer may be used for biomedical imaging/tomography
- Spectroscopic investigation of soft tissue
- THz is a unique tool for nano scale characterizations
  - Non-destrctive, Non-contact, sub-surface
  - Inspect 2D and 3D materials
  - Lattice defects, stacking faults
  - Defects, cracks, non-uniformity, inclusion, phases, etc.
- All non-metals: Semiconductors, laminates, etc.
- Both quantitative measurement and visual
- High sensitivity multispectral imaging and analysis
- Collaboration available and interested.

Thank you for your attention

Questions are welcome

Contact:

Anis Rahman

info@arphotonics.net

+1-717-623-8201